의학박사 학위논문

Membrane excitability of Purkinje cells in the vestibulocerebellum

전정소뇌 퍼킨지 세포의 세포막 흥분성

2013 년 4 월

서울대학교 대학원

의과학과 박사과정

김 창 희

A thesis of the Degree of Doctor of Philosophy

전정소뇌 퍼킨지 세포의 세포막 흥분성

Membrane excitability of Purkinje cells in the vestibulocerebellum

April 2013

The Department of Biomedical Sciences,
Seoul National University Graduate School
Chang-Hee Kim

Membrane excitability of Purkinje cells in the vestibulocerebellum

by
Chang-Hee Kim

A thesis submitted to the Department of Biomedical Sciences in partial fulfillment of the requirements for the Degree of Doctor of Philosophy in Medical Science at Seoul National University College of Medicine

April 2013

Approved by Thesis Committee:

Professor _____ **Chairman**

Professor _____ **Vice chairman**

Professor _____

Professor _____

Professor _____

ABSTRACT

Introduction: Cerebellar Purkinje cells (PCs) are the sole output of the cerebellar cortex, and function as key to a variety of learning-related behavior by integrating multimodal afferent inputs. Intrinsic membrane excitability of neuron determines the input-output relationship, and therefore governs the functions of neural circuits. Cerebellar vermis consists of ten lobules (lobule I-X), and each lobule receives different sensory information. However, lobule-specific differences of electrophysiological properties of PC are incompletely understood.

Methods: To address this question, we performed a systematic comparison of membrane properties of PCs from different lobules (lobules III-V *vs.* X) using patch-clamp technique.

Results: Two types of firing patterns (tonic firing and complex bursting) were identified in response to depolarizing current injections in lobule III-V PCs, whereas four distinct firing patterns (tonic firing, complex bursting, initial bursting and gap firing) were observed in lobule X. A-type K+ current and early inactivation of fast Na+ conductance with activation of 4-aminopyridine sensitive conductances were shown to be responsible for the formation of gap firing and initial bursting patterns, respectively, which were observed only in lobule X. In response to current injection, PCs in lobule X spiked with wider dynamic range.

Conclusions: These differences in firing pattern and membrane properties probably contribute to signal processing of afferent inputs in lobule-specific

fashion, and particularly diversity of discharge patterns in lobule X, as a part of vestibulocerebellum, might be involved in strict coordination of a precise temporal response to a wide range of head movements.

Keywords: Purkinje cell, intrinsic excitability, vestibulocerebellum,
Student number: 2008-31024

CONTENTS

LIST OF TABLES AND FIGURES

Chapter 1

Chapter 2

LIST OF ABBREVIATIONS

4-AP, 4-aminopyridine; ACSF, artificial cerebrospinal fluid; AHP, afterhyperpolarization; AP, action potential; CNS, central nervous system; CV, coefficient of variation; DCN, deep cerebellar nucleus; fAHP, fast afterhyperpolarization; GFN, gap firing neuron; HFF, high-frequency firing; I_A, A-type K^+ current; Ih, hyperpolarization-activated inward current; ISI, interspike interval; LFF, low-frequency firing; mGluR, metabotropic glutamate receptor; PC, Purkinje cell; sAHP, slow afterhyperpolarization; SFA, spike frequency adaptation; TFN, tonic firing neuron; VN, vestibular nucleus; TEA, tetraethylammonium chloride.

GENERAL INTRODUCTION

In the cerebellar vermis, each lobule receives different sensory information. Lobules III-V which are known as spinocerebellum receive major afferent input through ventral spinocerebellar tract, and lobule X which is known as vestibulocerebellum has extensive primary and secondary vestibular afferent. We hypothesized that Purkinje cells in different lobules may have different input-output functions with distinct membrane properties to encode different kinds of sensory modality. This study showed that intrinsic membrane properties vary widely between Purkinje cells in lobule III-V and X. Purkinje cells in lobule X exhibited more diverse firing patterns, and had wide dynamic range in their input-output curve not saturating their firing rates as readily as lobule III-V neurons. These findings are the first report, as far as we know, about the inter-lobular difference of intrinsic properties of Purkinje cells from the systematic comparison.

CHAPTER 1

Lobule-specific membrane excitability of cerebellar Purkinje cells

INTRODUCTION

It has been known that the cerebellum is a major associative center for sensory input, coordinates motor activity, and contributes to some higher cognitive functions, (1). Purkinje cells (PCs) lie in the center of this cerebellar circuitry. Information into the cerebellum enters via two principal afferent pathways: mossy fiber and climbing fiber. The mossy fiber-parallel fiber pathway and climbing fiber pathway converge in extensive dendritic arbors of PCs which are the sole output of the cerebellar cortex. A substantial volume of work about intrinsic properties of PCs has been done. In slice preparation *in vitro* where synaptic inputs have been blocked, PCs show spontaneous firing of action potentials (APs) (2). They also fire APs at high rates *in vivo* despite of the presence of spontaneous inhibitory synaptic activity into PCs (3). The changes in the pattern of PC activity are not only the result of synaptic input but mainly the alteration of intrinsic properties which are regulated by various ionic conductances in different cellular compartments (4, 5). During the first three weeks of postnatal development PCs undergo maturation in spontaneous firing activity, and intrinsic properties including Na^+-spike and Ca^{2+}-Na^+ spike firing complete maturation until postnatal day 18 (6).

Cerebellar vermis is subdivided into ten lobules, numbered I to X from rostral to caudal. Cerebellar cortex contains three layers (molecular, Purkinje, and granule cell layers), which is well conserved throughout lobules in the vermis. However, each lobule receives different sensory input, and may encode the information in functionally distinct fashion. Lobules III, IV, and V receive

major afferent input through ventral spinocerebellar tract which carries information from the hindlimbs (7). Lobule X which makes up a part of vestibulocerebellum has extensive vestibular input via primary and secondary vestibular afferent (8, 9).

As each lobule is considered to encode different kinds of sensory modality, PCs may have differences in the input-output function with distinct membrane properties according to their location in the cerebellar vermis. For example PCs of different lobules have other distinct characteristics such as expressional degree of certain transporters or receptors. PCs in lobule X express higher density of glutamate transporters than lobule III, which leads to a decrease in degree of mGluR activation and consequently makes lobule X PCs much less susceptible in forming synaptic plasticity (10). Interestingly, depolarization-induced slow current evoked by brief strong depolarization were more prominent in lobules IX, X than lobules II, III, V, VI, which may be related to higher expression of molecules involved in dopamine signaling such as D_3 dopamine receptors in PCs of lobule IX, X (11). However, little is known about the difference in membrane properties of PCs within different lobules. In the present study, we compared intrinsic membrane properties of cerebellar PCs between lobule III-V and X to investigate if afferent information is encoded in a lobule-specific way by differential discharge properties. We used the whole cell patch-clamp technique to record membrane properties from PCs of different lobules. We found that PCs in lobule III-V and X display different characteristics in their responses to hyperpolarizing and depolarizing current injections.

MATERIALS AND METHODS

1. Slice preparation

All animal use was in accordance with protocols approved by the Institution's Animal Care and Use Committee of Seoul National University College of Medicine. Rats were anaesthetized by isoflurane inhalation and decapitated. Parasagittal slices of the cerebellar vermis (300 μm thick) were prepared from P21–P23 Sprague-Dawley rats using a vibratome (Microm HM 650V, Germany). The slices were taken approximately 500 μm to both sides of the midline, and ice-cold standard artificial cerebrospinal fluid (ACSF) containing 124mM NaCl, 2.5mM KCl, 1mM Na_2HPO_4, 1.3mM $MgCl_2$, 2.5mM $CaCl_2$, 26.2mM $NaHCO_3$, and 20mM D-glucose, bubbled with 95% O_2 and 5% CO_2. After cutting, slices were kept for 30min at 35℃ and then for up to 8hr at 25℃ in ACSF.

2. Whole cell patch-clamp recordings

After a recovery period, the slices were transferred to a submerged chamber on the stage of a Olympus BX 50WI microscope (Olympus Optical, Tokyo, Japan) and kept in place with a nylon-strung platinum harp. The tissue was continuously perfused with ACSF at a rate of 2ml/min. 100 μM picrotoxin (Sigma, St. Louis, MO, USA) and 1mM kynurenic acid (Sigma, St. Louis, MO, USA) were added to the perfusate to block the GABAergic and ionotropic glutamatergic synaptic inputs to the PCs. Somatic whole-cell current-clamp recordings were obtained from PCs in lobule III-V and lobule

X (Fig. 1*E*). The series resistance was usually between 11 and 15 MΩ. All data were recorded using an EPC-9 patch-clamp amplifier (HEKA Elektronik, Germany) with sampling frequency of 20 kHz, and the signals were filtered at 2 kHz. Glass pipettes (2–4 MΩ) were filled with internal solution containing (in mM): K gluconate 135, NaCl 7, MgATP 2, NaGTP 0.3, HEPES 10, EGTA 0.5, phosphocreatine di(tris) salt 10, pH 7.2. Recordings were performed at 30 ℃. Recordings were started 5 min after obtaining the whole-cell configuration to allow diffusion of the internal solution into the cytosol. Some experiments were performed under voltage-clamp mode. The external solution used during voltage-clamp recordings was prepared omitting $CaCl_2$ but containing 3.8 mM $MgCl_2$, 100 μM EGTA, 200 μM $NiCl_2$, 125 μM $CdCl_2$, and 1 μM tetrodotoxin to block voltage-dependent Ca^{2+} and fast Na^+ channel and isolate K^+ currents.

3. Data measurement and analysis

Data were acquired by Pulse software (HEKA Elektronik, Germany) and analyzed offline with the program IgorPro (Wavemetrics, Lake Oswego, OR, USA). Neuronal responses were studied at membrane potential of -70 mV to minimize the influence of voltage dependent changes on membrane conductance. Neurons in which the holding current was greater than 400 pA were discarded from analysis. Hyperpolarizing and depolarizing current injections (from -600 pA to +1000 pA with increments of 100 pA) of 1 s duration were applied with a step interval of 5 s and each series was repeated for three trials. Parameters of neuronal responses to current injection were

analyzed to evaluate the PC excitability. Input resistance was determined by measuring the maximal voltage deflection during hyperpolarizing current injection (the difference between the baseline before the current step and the maximal negative voltage reached during the hyperpolarizing current injection) (12). Values from three trials with current steps to intensities from -600 pA to -300 pA were averaged (Figure 1-1A). The amount of the contribution of the inward rectifying cationic current (sag amplitude) was determined as the average of difference between the maximal negative voltage and the plateau voltage deflection from hyperpolarizing current injection of -600 pA (Figure 1-1A) (13). Membrane capacitance (C_m) was measured from $C_m=\tau/R$, at which the time constant (τ) and series resistance (R) were calculated by exponential curve fit of response to hyperpolarizing voltage steps (-5 mV) from a holding potential of -70 mV. Rheobase, the minimum current magnitude required to produce an action potential (AP) was estimated by injection of current steps in 5 pA increments. The voltage threshold was determined from the first AP at rheobase by measuring the membrane potential at which d*V*/d*t* first entered within the range 30–60 mV/ms (14). The AP amplitude was measured from the same spike as the difference between the peak and the threshold voltage. The amplitude of AP afterhyperpolarization (AHP) was measured as the difference between the AP threshold and the negative peak of AHP (Figure 1-1B, upper trace). The maximal upstroke velocities of AP were obtained from the same spike by measuring peak values of d*V*/d*t* (Figure 1-1A, lower trace). Spike-train duration during depolarizing current injection was determined as the

difference in time between the first and last spike (Figure 1-1A, upper trace). Initial firing rate was defined as the frequency of initial five spikes during current injection (Figure 1-1A, lower trace). Initial firing rate and spike-train duration of Ca^{2+}-Na^{+} bursts in complex bursting neuron were measured as average of traces. Data are expressed as mean ± SEM and '*n*' indicates the number of neurons tested. Statistical evaluations were performed using *t*-test (in some cases, nonparametric Mann-Whitney test) and one-way ANOVA with *post hoc* Scheffe's test. $P < 0.05$ was considered to be significant.

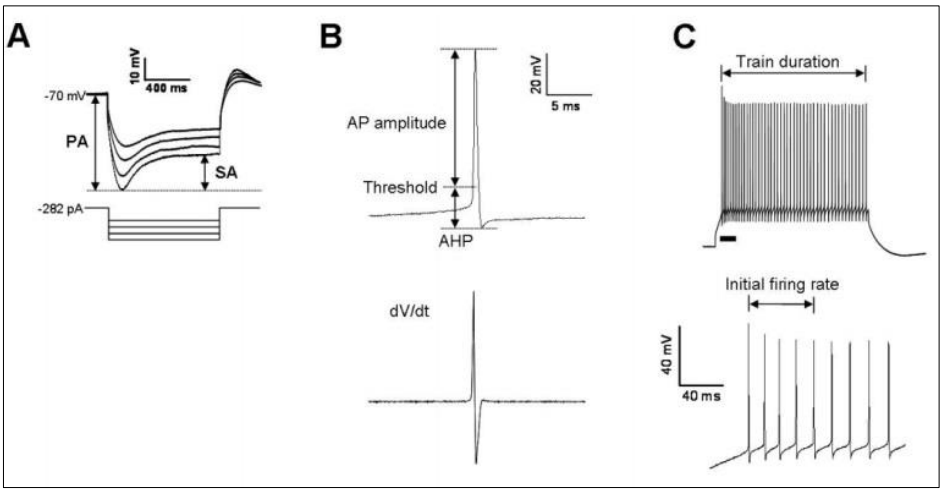

Figure 1-1. Overview of evoked response parameters

(**A**) Input resistance was determined by measuring the maximal voltage deflection (peak amplitude, PA) during hyperpolarizing current injection. Values from three trials with current steps to intensities between -600 pA and -300 pA were averaged. The amount of the contribution of the inward rectifying cationic current was calculated as the difference between the maximal negative voltage and the plateau voltage deflection (sag amplitude, SA). Measurements were performed with hyperpolarizing current injections of -600 pA and averaged. Bottom traces, injected currents (superimposed). (**B**) The voltage threshold of action potential was measured from the first spike of the rheobase current injection (upper trace), which was determined as the first point where the velocity (dV/dt, lower trace) entered within the range of 30-60 mV/ms. (**C**) Depolarizing current injections of constant length of 1s were used to evoke spike-train responses. Spike duration was defined as the difference in time between the first and last action potentials (upper trace).

Initial firing rate during evoked spike-trains was estimated as the mean frequency over the first five spikes (lower trace).

RESULTS

Lobule-specific differences in firing patterns

We used whole-cell patch-clamp technique in PCs of lobule III-V and X (Figure 1-2E), and divided the population of neurons into four categories according to their firing pattern in response to 1 s depolarizing current injections. Tonic firing neurons were characterized by continued discharge of APs in response to depolarizing current commands. Tonic cells exhibited higher firing frequency in response to increasing current intensity until the occurrence of Na^+ spike failure (Figure 1-2A).

Complex bursting neurons showed sustained Na^+ spike discharge by low-intensity depolarizing current injection. However, a rapid failure of Na^+ spikes and the onset of Ca^{2+}-Na^+ bursts were observed by injecting higher depolarizing current (Figure 1-2B). Each Ca^{2+}-Na^+ burst consists of Na^+ spike bursts and Ca^{2+} spike which terminates the Ca^{2+}-Na^+ burst, as observed in our study (Figure 1-2B and 7). Subsequent burst of Na^+ spikes appears immediately after the Ca^{2+} spike of which deep AHP makes membrane potential hyperpolarized recovering Na^+ channel from inactivation. Previous studies using freshly prepared cerebellar slices of rats and mice have reported that PCs show only tonic firing or complex bursting patterns in response to depolarizing current injection (14-17).

Initial bursting neurons were defined as those that exhibited only one or a few spikes at the beginning of the depolarizing current injection and remained silent during the remainder of the current pulse (Figure 1-2C). These neurons

are not able to fire at steady-state discharging transient spikes which were followed by a long plateau potential. It has been reported that this plateau potential represents an unstable equilibrium state involving at least three simultaneously occurring voltage-dependent conductances: non-inactivating Na^+ conductance, non-inactivating K^+ conductance, and dominant Ca^{2+}-dependent component (12). This firing pattern has been observed in PCs from organotypic cerebellar slice cultures (18, 19), but not in PCs from acute slice preparations.

Gap firing neurons were characterized by a delay between the onset of the current injection and the first AP which is of shorter height than successive spikes when just suprathreshold currents were injected. They also showed a slow ramp depolarization in response to subthreshold depolarizing current injections. When the stronger current pulses were applied, the first spike was generated with no delay followed by a long first interspike interval. The gap between first and second spikes was successively shortened with increasing current intensity, and with high-intensity current pulse no gap was generated (Figure 1-2D). Gap firing pattern has been reported in several neuron types in spinal cord, superior colliculus and vagal motoneurons (20-22), but as far as we know it has not been reported in PCs yet.

Firing patterns were not uniformly distributed in lobule III-V and X (Figure 1-2F and G). Tonic firing neurons and complex bursting neurons were found both in lobule III-V and X. In contrast, gap firing and initial bursting neurons were encountered only in lobule X. Tonic firing neurons and complex bursting neurons were found in 68% (n = 25) and 32% (n = 12) of neurons,

respectively in lobule III-V. In lobule X, 27% of neurons were tonic firing (*n* = 13), 22% were complex bursting (*n* = 11), 20% were initial bursting (*n* = 10), and 31% were gap firing neurons (*n* = 15).

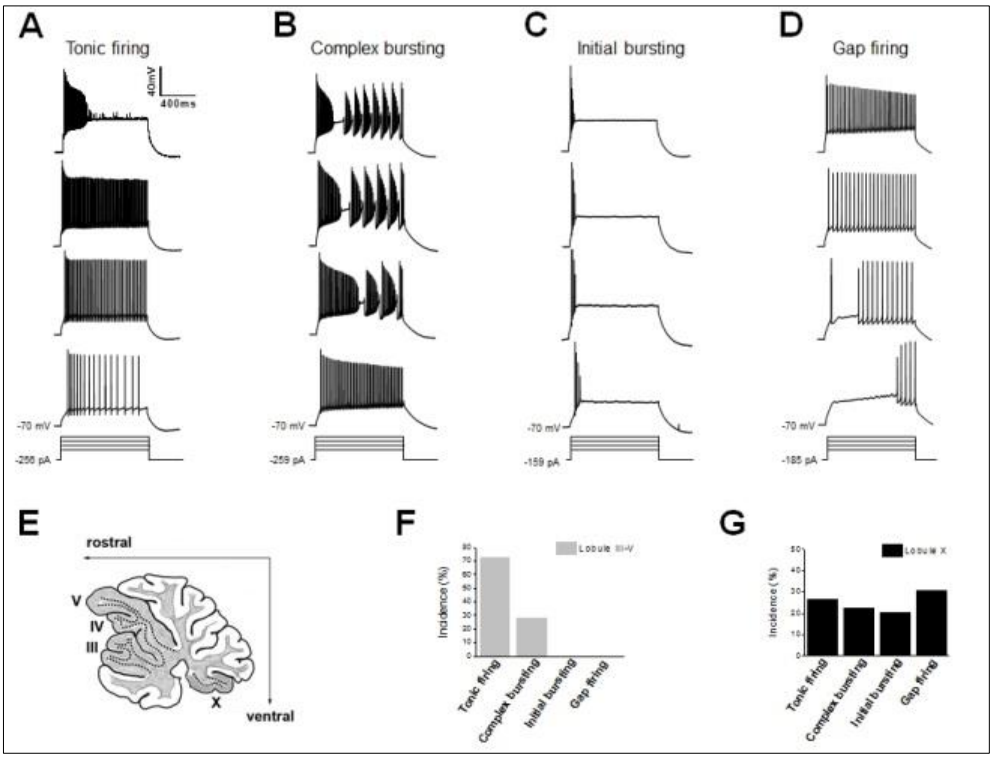

Figure 1-2. Firing patterns of Purkinje neurons in cerebellar vermis

Firing patterns were determined in response to depolarizing currents injected from hyperpolarized holding potentials. Representative traces are shown: Tonic firing (**A**), complex bursting (**B**), initial bursting (**C**), and gap firing pattern (**D**). Bottom traces, injected currents (superimposed). *E*, Schematic illustration of a cerebellar vermis in parasagittal plane showing lobules III, IV, V and X (thicker dotted line). Differential distribution of firing patterns in lobule III-V (*F*, n = 37), and X (*G*, n = 49). Percentages of neurons with the each firing pattern are shown.

Mechanisms underlying gap firing and initial bursting pattern

The characteristic delay between the onset of current injection and the first AP were observed when lower-intensity current pulses were injected from holding potential of -70 mV or more negative potentials (Figure 1-3A, middle trace). When higher-intensity current pulses were applied, first AP was generated with no delay followed by a long gap between first and second spikes (Figure 1-3A, top trace). However, tonic firing pattern was elicited in the same neuron when the current pulse was injected from more positive holding potentials suggesting voltage-dependent inactivation of transient outward current (n = 5, Figure 1-3B). High concentration 4-aminopyridine (4-AP, 5 mM) was added to bath solution in five experiments to block A-type K^+ current (I_A) (23). The delay to the first AP and a characteristic gap between the first and second spikes disappeared, and tonic firing pattern was observed even when evoked from hyperpolarized holding potentials (Figure 1-3C). Application of 50-100 nM dendrotoxin-I, antagonist of D-type K^+ current, showed no effect on firing patterns of gap firing neurons (Data not shown). These results suggest that I_A may be responsible for the generation of gap firing pattern in PCs of lobule X.

To examine the outward currents activated by depolarizing input, voltage-clamp recordings were performed perfusing Ca^{2+}-free bath solution in the presence of synaptic and certain ion channel blockers (see Materials and Methods). To better isolate I_A, tetraethylammonium chloride (TEA, 4 mM) was added to the bath solution to block K^+ currents of delayed rectifier type. To examine I_A in gap firing neurons, gap firing pattern was first identified

under current-clamp mode, and then voltage-clamp recordings were performed after changing external solution (Figure 1-3D). Outward K^+ currents were elicited by 2 s depolarizing steps to potentials between -80 and +20 mV with 10 mV increments and 10 s intervals from a holding potential of -90 mV. In control recordings, the amplitude of I_A current was increased with depolarization (Figure 1-3D, top trace). Adult PCs are large cells with extensive dendritic arborizations, so the high-quality voltage control is difficult to achieve. Although this space-clamp problems would significantly affect the voltage-dependence and time course of the 4-AP sensitive currents, we could observe 3mM 4-AP completely blocked I_A (n = 3; Figure 1-3D), which is consistent with the observation under the current-clamp mode in which high concentration 4-AP abolished the gap in gap firing neurons (Figure 1-3C). I_A with slower kinetics was shown to be responsible for the formation of gap firing pattern. I_A is a transient voltage-dependent outward K^+ current that counteracts fast depolarization and thus leads to a delayed onset of firing making more positive AP threshold. When stronger current pulses are applied, the slow activation of I_A allows just one AP to be generated before a long gap at the onset of current injection. To rule out the possibility that other types of K^+ currents may contribute to the formation of gap firing pattern, we repeated the experiments with different K^+ channel blockers such as TEA, iberiotoxin (large-conductance Ca^{2+}-activated K^+ channel blocker), and apamin (small-conductance Ca^{2+}-activated K^+ channel blocker) (Figure 1-4). It is known that 80-90% of Kv3 channel activity is blocked by 1 mM TEA (22), and the typical gap in gap firing neurons did not disappear at this

concentration (n = 3, data not shown). TEA has been reported to block Kv2.1 with an IC_{50} of ~5 mM (24, 25), and gap firing was still observed after the application of 5 mM TEA (n = 5, Figure 1-4A). Bath application of 100 nM iberiotoxin (15) did not eliminate the typical gap between first and second AP in gap firing neurons (n = 6, Figure 1-4B). Gap firing was still observed after the application of 100 nM (5) apamin (n = 4, Figure 1-4C).

Detailed characterization of initial bursting neurons which were observed only in lobule X PCs was performed. The characteristic transient spikes were shown when depolarizing current was injected from holding potential of -70 mV (n = 10, Figure 1-5A). To examine the possible involvement of rapid inactivation of fast Na^+ channels, additional current was injected during a maintained current step. The additional current injection was not able to elicit spikes no matter how high intensity of current was injected (Figure 1-5B), suggesting that fast Na^+ conductances were already inactivated. 4-AP sensitive K^+ conductance has been postulated to be responsible for the initial bursting in neurons of mammalian cochlear nucleus or medial nucleus of trapezoid body and avian nucleus magnocellularis (26-28). When 1 mM 4-AP was added to the bath, depolarizing current injection elicited a train of repetitive bursts (n = 3, Figure 1-5C), which imply that 4-AP sensitive conductances exert a great influence on the formation of initial bursting pattern in lobule X.

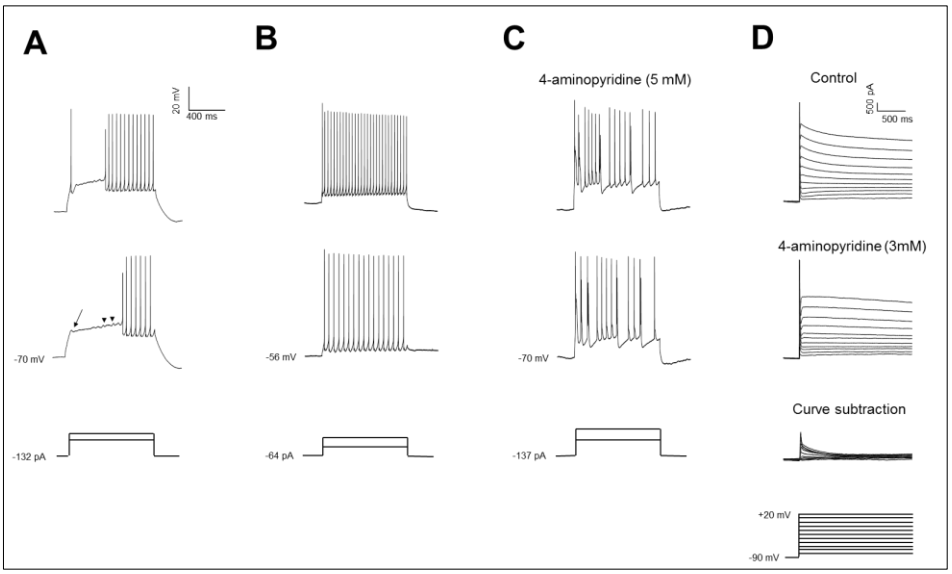

Figure 1-3. Examination of electrophysiological properties of gap firing neurons

(**A**) Membrane potential was held at -70 mV by injecting -132 pA. A characteristic delay between the onset of current step and the first spike was observed when low depolarizing current pulses were injected from this hyperpolarized holding potential (middle trace). Note that a slow ramp-like depolarization is observed during the period between the onset of current injection and the first spike. A transient hyperpolarization occurred following the onset of the membrane depolarization (arrow), and clusters of spikes were interrupted by subthreshold membrane oscillations (arrowheads). When the higher current pulses were applied, the first spike was elicited with no delay but a long first interspike interval was observed (top trace). (**B**) The neuron was held at -56 mV by injecting -64 pA. Depolarizing current pulses evoked a tonic firing pattern at this depolarized holding potential. (**C**) No delay was observed from the onset of current injection to the first spike when 5 mM 4-aminopyridine (4-AP) was applied. Bottom traces, injected currents (superimposed). (**D**) Activation of transient K^+ current was assessed by 2 s depolarizing steps to potentials between -80 and 20 mV with 10 mV

increment from holding potential of -90 mV. In this recording of I_A, 4 mM TEA was applied to block most non-inactivating K^+ currents. I_A amplitude was increased with incremental depolarizing commands. Application of high concentration (3 mM) 4-AP abolished I_A. The amount of remaining delayed K^+ current was still large. The amount of I_A was measured by subtracting the curves under 4-AP from the control curves.

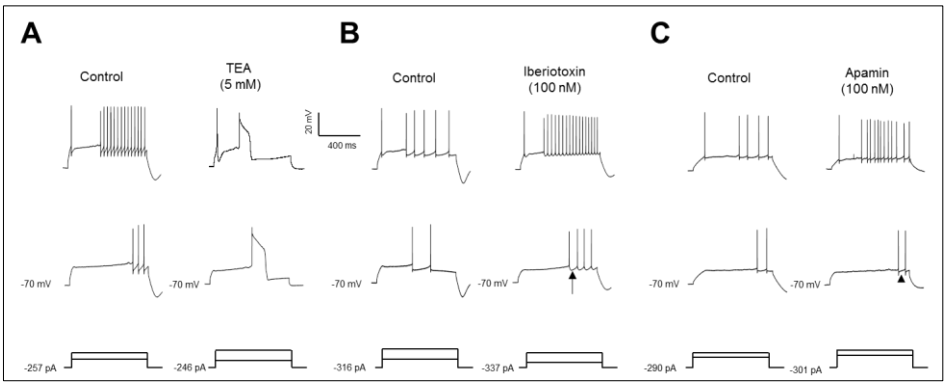

Figure 1-4. Effect of TEA, iberiotoxin and apamin on gap firing neruons

K^+ channel blockers including tetraethylammonium (TEA), iberiotoxin (blocker of large-conductance Ca^{2+}-activated K^+ channel) and apamin (blocker of small-conductance Ca^{2+}-activated K^+ channel) were perfused to examine if K^+ conductance other than I_A may influence the electrophysiological properties of gap firing neurons. Typical gap between the first and second spike is still present after application of 5 mM TEA (*n* = 5, **A**). (**B**) Gap firing was still observed after perfusion of iberiotoxin (100 nM, *n* = 6). Note that the change in the shape of afterhyperpolarization (AHP, arrow) is shown due to the effect of iberiotoxin. (**C**) Apamine (100 nM) did not eliminate the typical gap in gap firing neurons (*n* = 4). The change of AHP shape (arrowhead) and irregular firing (top trace) were notable. Bottom traces, injected currents (superimposed).

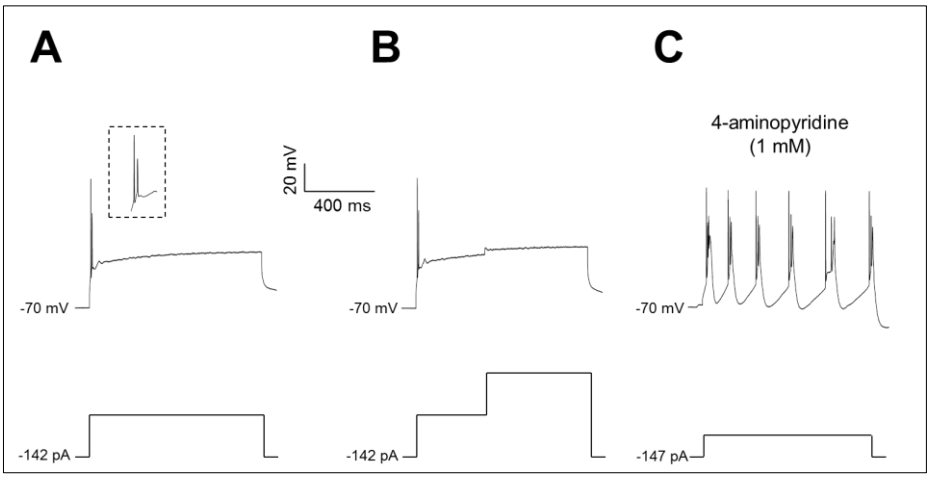

Figure 1-5. Electrophysiological properties of initial bursting neurons

(**A**) Representative trace of initial bursting neuron. Only transient burst of spikes was generated by the depolarizing current step. Compared with the first spike, subsequent spike has lower AP amplitude and higher AP threshold (inset). (**B**) Additional current injection during an active depolarizing current step did not generate any spike. (**C**) After application of 1 mM 4-AP, a train of repetitive bursts was elicited in response to depolarizing current injection in the same cell. Bottom traces, injected currents.

Passive and active membrane properties of PCs from lobule III-V and X

PCs from different lobules showed significant differences in most of parameters of membrane properties examined. These results are summarized in Table 1-1. Input resistance and magnitude of inward rectification were evaluated to assess passive membrane properties using hyperpolarizing current injection. Negative current injection evoked voltage deflection which consisted of negative bump followed by a short rising phase and a plateau (Figure 1-1A). Initial negative voltage bump is due to passive response of the membrane. After reaching peak deflection it changes direction into depolarization when hyperpolarization-activated inward current (Ih) is activated. In this study the peak amplitude of negative voltage deflection was used to measure the input resistance, since at this time the contribution of Ih is still minimal (29). The measures were taken with four different intensities of current injection and repeated for three trials to better estimate the input resistance. PCs in lobule III-V showed significantly higher input resistance (102.6 ± 6.5 MΩ, n = 37) than PCs in lobule X (89.7 ± 5.3 MΩ, n = 49, Table 1). Input resistance of tonic firing neurons in lobule III-V (101.9 ± 6.4 MΩ, n = 25) differed significantly from that of tonic firing neurons in lobule X (75.6 ± 4.2 MΩ, n = 13, Figure 1-6A), but was not different from that of gap firing neurons in lobule X (101.8 ± 4.8 MΩ, n = 15). Input resistance is determined chiefly by resistance of the membrane, which is related to neuronal size, shape and resting membrane conductance. Input resistance of PCs has been demonstrated to decrease dramatically over the first 15 postnatal

days and reaches adult levels by postnatal day 18 (6). Previous studies have reported that input resistance can be increased by long term synaptic potentiation and during retention of learning (30, 31). Our results demonstrated that input resistance was significantly different between PCs of lobule III-V and lobule X, which indicates that PCs of lobule III-V and X may have different size, shape or resting membrane conductance. To investigate the effect of 4-AP-sensitive current on input resistance, we measured input resistance after the application of 5 mM 4-AP. In the presence of 5 mM 4-AP, input resistance was not significantly changed in both lobule III-V (105.2 ± 20.1 MΩ to 106.8 ± 15.9 MΩ for tonic firing neurons, n = 4 and 110.7 ± 17.1 MΩ to 111.2 ± 20.0 MΩ for complex bursting neurons, n = 3) and lobule X PCs (73.8 ± 13.8 MΩ to 70.1 ± 11.9 MΩ for tonic firing neurons, n = 4 and 96.3 ± 14.2 MΩ to 91.7 ± 15.4 MΩ for complex bursting neurons, n = 2) (Figure 1-7, top traces). Since the membrane behavior of PCs is highly influenced by Ih current at subthreshold potentials, the contribution of Ih current to input resistance was examined. Bath application of selective Ih blocker, ZD 7288 (10 μM) (13) completely abolished sag (Figure 1-7, middle traces), and led to a significant increase in the input resistance in both lobule III-V (100.6 ± 15.9 MΩ to 148.8 ± 13.4 MΩ for tonic firing neurons, n = 3 and 103.7 ± 17.2 MΩ to 183.3 ± 19.2 MΩ for complex bursting neurons, n = 3) and lobule X neurons (72.7 ± 14.7 MΩ to 114.9 ± 15.2 MΩ for tonic firing neurons, n = 4 and 89.2 ± 15.9 MΩ to 135.6 ± 12.3 MΩ for complex bursting neurons, n = 4), which was similar to previous observations by other

researcher (32). Lobule X PCs showed significantly larger membrane capacitance than lobule III-V neurons (670.6 ± 22.1 pF, *n* = 49 *vs.* 560.1 ± 25.1 pF, *n* = 37, Table 1-1). Membrane capacitance of tonic firing neurons and complex bursting neurons in lobule X was significantly larger than neurons in lobule III-V (Figure 1-6B). The fact that lobule X PCs have higher membrane capacitance but lower input resistance may indicate that there is higher resting K^+ conductance in lobule X neurons. Further evaluation of morphologic differences between PCs from lobule III-V and X remains to be elucidated.

The amplitude of the shift from peak voltage deflection to plateau was used to measure the magnitude of inward rectification. The amplitude of inward rectification was 17.0 ± 1.0 mV and 22.6 ± 1.4 mV in PCs of lobule III-V (*n* = 37) and lobule X (*n* = 41), respectively, and the ratio of sag amplitude to peak amplitude was significantly lower in lobule III-V PCs (0.31 ± 0.01, *n*=37) than lobule X PCs (0.46 ± 0.01, *n*=41). Ih current consists of a slowly developing mixed inward current carried by K^+ and Na^+ that is activated by hyperpolarization more negative than -65 mV, (33). In acutely dissociated PCs, inward current through Ih channel was negligible at membrane potential near AP threshold, and frequency of tonic AP was not altered by pharmacological blockade of Ih (34). Ih can modify the pattern of spontaneous burst generation (29), and control tonic AP firing by maintaining membrane potential bistability (13).

Active membrane properties were assessed by injection of depolarizing current. In this study we measured AP threshold, amplitude, and maximal d*V*/d*t* of spike upstroke from the first AP evoked by rectangular current steps in 5 pA increments. Regarding voltage threshold of AP, neurons in lobule III-V displayed a more negative potential (-44.6 ± 0.7 mV, *n* = 37) than in lobule X (-34.6 ± 1.3 mV, *n* = 49) (Table 1-1, Figure 1-6C). Rheobase current, AP amplitude, and maximal d*V*/d*t* were significantly different between neurons in lobule III-V and X (Table 1-1). Examination of the waveforms and the properties of the first AP at rheobase revealed apparent differences between lobule III-V and lobule X neurons (Figure 1-8, top traces). AP threshold was significantly higher in PCs of lobule X than lobule III-V (Table 1-1, Figure 1-6C). The voltage trajectory (d*V*/d*t*) versus time (Figure 1-8, middle traces), as well as phase plot of d*V*/d*t* versus voltage (Figure 1-8, bottom traces) of the first AP of neurons in lobule III-V showed apparent differences compared with those in lobule X. AHP amplitude was not significantly different between PCs in lobule III-V and X. However, as observed in previous study (35), AHP amplitude of gap firing neurons in lobule X (19.6 ± 0.9 mV, *n* = 15) was significantly higher than tonic firing neurons in lobule III-V (12.2 ± 0.6 mV, *n* = 25) or tonic firing neurons in lobule X (11.4 ± 1.1 mV, *n* = 13), which may partially be accounted for the high AP threshold due to subthreshold activation of I_A in gap firing neurons. Tonic firing and gap firing neurons in lobule X did not show significant difference between each other in train duration and initial firing rate.

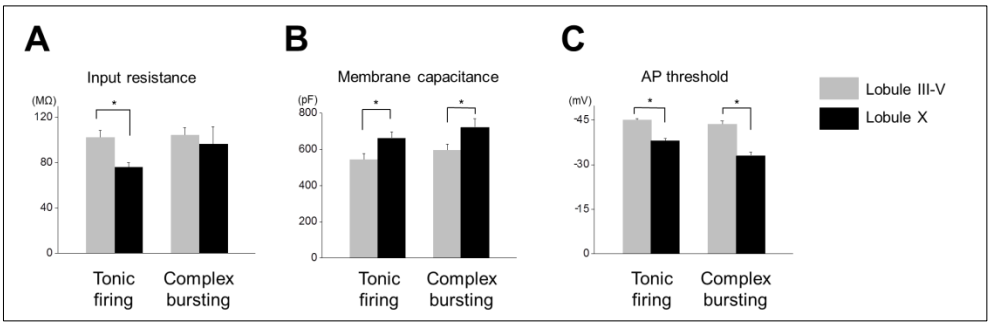

Figure 1-6. Comparison of input resistance, membrane capacitance, and AP threshold between lobule III-V and lobule X neurons

Input resistance was significantly higher in lobule III-V tonic firing neurons than lobule X (**A**, 101.9 ± 6.4, *n* = 25 *vs*. 75.6 ± 4.2, *n* = 13). Membrane capacitance was significantly lower in lobule III-V than lobule X for both tonic firing (**B**, 543.7 ± 32.9 *vs*. 661.8 ± 36.2) and complex bursting neurons (*B*, 596.1 ± 34.0, *n* = 12 *vs*. 721.9 ± 46.9, *n* = 11). Lobule III-V neurons showed lower action potential (AP) threshold than lobule X neurons (**C**, -45.1 ± 0.5 *vs*. -43.6 ± 1.2 for tonic firing neurons and -38.0 ± 0.9 *vs*. -33.1 ± 1.1 for complex bursting neurons).

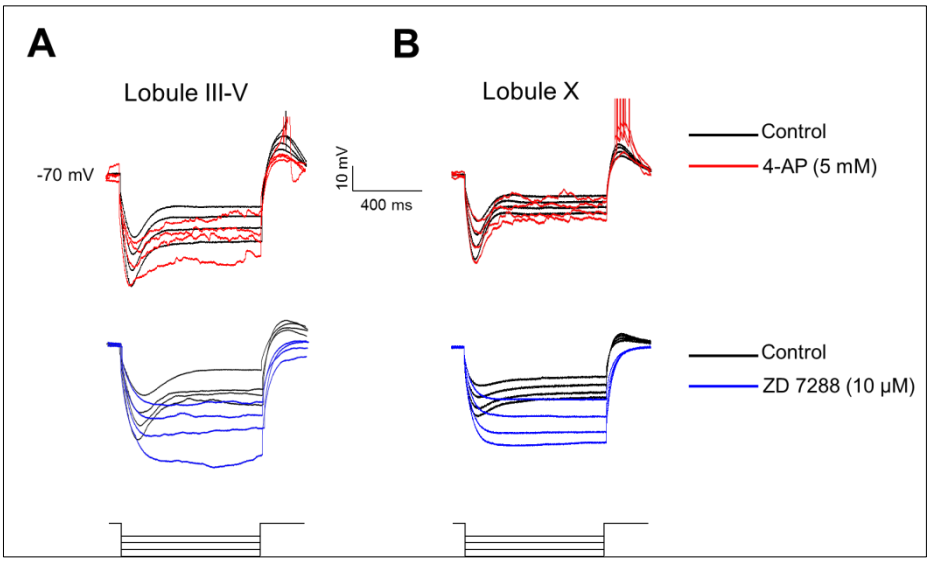

Figure 1-7. Effect of 4-aminopyridine and ZD 7288 on input resistance of Purkinje cells

Four hyperpolarizing current injections (-600 pA to -300 pA, see Materials and Methods) were done to measure input resistance under control conditions and in the presence of 5 mM 4-aminopyridine (4-AP, red color) or 10 μM ZD 7288 (blue color). Representative traces are shown. Application of 4-AP showed no significant change in the amplitude of maximal negative voltage deflection elicited by hyperpolarizing current injection in neurons of both lobule III-V and X (**A** and **B**, top traces). Blocking Ih by ZD 7288 caused a dramatic increase in input resistance and eliminated sag during hyperpolarizing current injection (**A** and **B**, middle traces). Bottom traces, injected currents (superimposed).

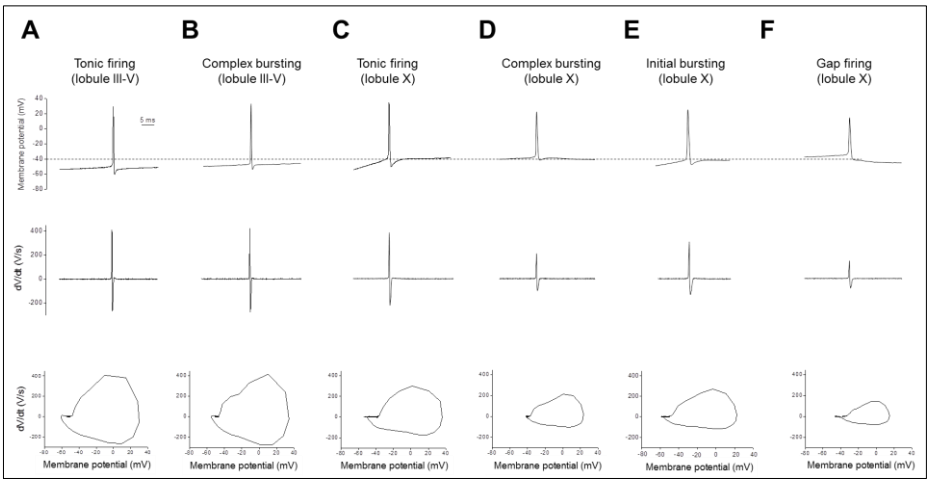

Figure 1-8. Waveform and properties of Na^+ spikes in Purkinje cells (PCs) of different firing patterns

Representative plots of action potential (AP) of tonic firing in lobule III-V (**A**), complex bursting in lobule III-V (**B**), tonic firing in lobule X (**C**), complex bursting in lobule X (**D**), initial bursting in lobule X (**E**), and gap firing in lobule X (**F**), respectively (upper trace). Each representative AP was the first AP observed by injection of current steps in 5 pA increments. Representative plots of dV/dt vs. time (middle trace) and phase plots of dV/dt vs. voltage (lower trace).

Table 1-1. Passive and active membrane properties of Purkinje neurons from different lobules.

	Lobule III-V (n = 37)		Lobule X (n = 49)			
	Tonic firing (n = 25)	Complex bursting (n = 12)	Tonic firing (n = 13)	Complex bursting (n = 11)	Initial bursting (n = 10)	Gap firing (n = 15)
Input resistance (MΩ)*	101.9 ± 6.4	104.2 ± 6.7	75.6 ± 4.2†	96.2 ± 15.5	87.8 ± 4.4	101.8 ± 4.8§
Sag amplitude (mV)*	16.4 ± 0.8	18.4 ± 1.5	21.0 ± 1.3†	21.8 ± 0.7‖	24.1 ± 1.9	23.2 ± 1.3‡
Membrane capacitance (pF)*	543.7 ± 32.9	596.1 ± 34.0	661.8 ± 36.2†	721.9 ± 46.9‖	681.1 ± 46.8	618.9 ± 50.9
AP threshold (mV)*	-45.1 ± 0.5	-43.6 ± 1.2	-38.0 ± 0.9†	-33.1 ± 1.1‖	-39.7 ± 1.7	-28.5 ± 1.3‡,§
Rheobase current (pA)*	112.6 ± 13.8	116.3 ± 9.6	295.4 ± 28.4†	246.7 ± 46.6‖	280.0 ± 32.6	283.3 ± 34.4‡
AP amplitude (mV)*	77.3 ± 1.3	74.6 ± 2.2	68.6 ± 2.0†	56.0 ± 1.8‖	64.4 ± 1.3	37.7 ± 3.1‡,§
Maximal dV/dt, upstroke (V/s)*	405.9 ± 12.5	392.6 ± 17.4	314.1 ± 14.3†	245.0 ± 9.0‖	283.2 ± 13.5	114.4 ± 16.5‡,§
AHP (mV)	12.2 ± 0.6	10.7 ± 0.6	11.4 ± 1.1	10.5 ± 1.7	13.5 ± 1.5	19.6 ± 0.9‡,§

Statistical significance was examined by unpaired t-test or one-way ANOVA with *post hoc* Scheffe's test.

n = number of observations.

Statistical comparison of parameters was first performed in all neurons irrespective of firing pattern between lobule III-V and X.

*$P < 0.05$ between Purkinje neurons of all firing patterns in lobule III-V and those in lobule X.

Then, statistical comparison was done among tonic firing neurons in lobule III-V, tonic firing neurons in lobule X, and gap firing neurons in lobule X.

†$P < 0.05$ between tonic firing neurons in lobule III-V and tonic firing neurons in lobule X.

‡$P < 0.05$ between tonic firing neurons in lobule III-V and gap firing neurons in lobule X.

[§] $P < 0.05$ between tonic firing neurons in lobule X and gap firing neurons in lobule X.

[‖] $P < 0.05$ between complex bursting neurons in lobule III-V and complex bursting neurons in lobule X.

Comparison of repetitive Na^+ spikes in response to depolarized current injection in PCs from lobule III-V and X

Voltage responses induced by depolarizing current injection were compared in PCs from lobule III-V and X. Representative recordings of evoked activity from tonic firing neurons in lobule III-V (Figure 1-9A), tonic firing neurons in lobule X (Figure 1-9B), and gap firing neurons in lobule X (Figure 1-9C) are shown. As can be expected from lower rheobase current, tonic firing neurons in lobule III-V generated Na^+ spike trains at lower depolarizing-current injection than lobule X neurons. Continuous spike firing was evoked by sufficient depolarization both in tonic firing and gap firing neurons in lobule X. Strong depolarizing current injection caused failure of Na^+ spike followed by complete block of firing and the appearance of plateau potentials. Train duration which is defined as the time period between the first and the last spike, peaked at lower current injection in tonic firing neurons in lobule III-V than in tonic and gap firing neurons in lobule X (Figure 1-9D). In these three groups of neurons, initial firing rate was increased as higher depolarizing currents were injected, and the slope of increase of tonic firing neurons in lobule III-V was steeper than neurons in lobule X (Figure 1-9E).

Neurons with complex bursting pattern generated trains of Na^+ spikes in response to lower-intensity depolarizing current injection. However, as the intensity of the injected current increases, Na^+ spike failure occurs rapidly and PCs shift into a Ca^{2+}-Na^+ burst output. Each burst consists of a series of Na^+ spikes terminated by a Ca^{2+} spike (12, 36). This pattern of complex bursting was observed both in lobule III-V and X (Figure 1-10A and B). Neurons in

lobule III-V generated Ca^{2+}-Na^{+} bursts at lower depolarizing-current injection compared to neurons in lobule X. As the higher-intensity currents are injected, neurons showed increased number of bursts with shorter duration (Figure 1-10A and B). Average burst duration and initial firing rate were compared between neurons in lobule III-V (Figure 1-10A) and lobule X which showed tonic firing pattern when low-intensity currents were injected (Figure 1-10B). The average burst duration which is defined as the averaged time period between the first and the last intraburst spike, peaked at lower current injection in neurons in lobule III-V than in lobule X (Figure 1-10C). Initial firing rate was increased as the higher-depolarizing currents were injected in neurons of both lobule III-V and lobule X, and the slope of increase was steeper in neurons of lobule III-V (Figure 1-10D).

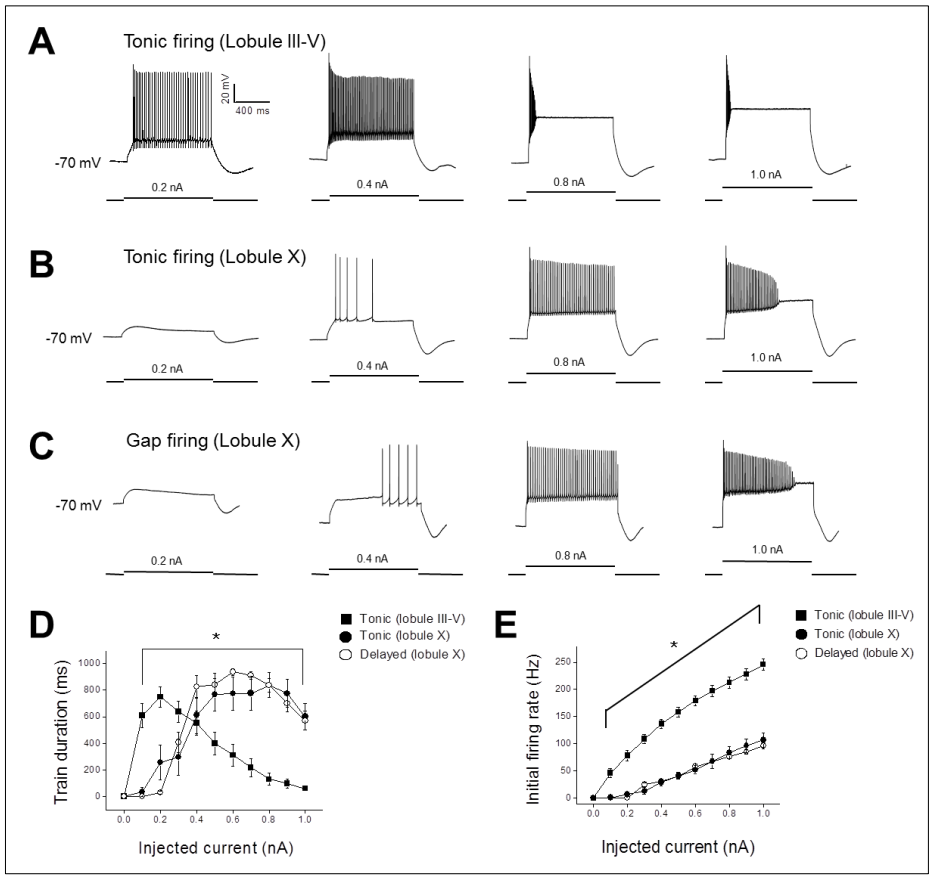

Figure 1-9. Comparison of electro-responsiveness of tonic and gap firing neurons in different lobules by depolarizing current injection

Representative voltage responses evoked in tonic firing neurons in lobule III-V (**A**), tonic firing neurons in lobule X (**B**), and gap firing neurons in lobule X (**C**) by depolarizing current-pulses of increasing size (left to right). Compared with tonic firing neurons (**B)** or gap firing neurons (**C**) in lobule X, lobule III tonic neurons (A) fired action potentials at smaller current injection and showed Na^+ spike failure earlier when larger amount of current was injected. (**D)** Summary plot showing train duration vs. injected current. Duration of repetitive firing was increased in response to higher depolarizing current injection within low-intensity range. Train duration was decreased with injection of highly depolarizing currents as failure of Na^+ spike occurred. (**E)**

Collected results displaying initial firing rate vs. injected current in neurons. Higher initial firing rate was obtained with current injection of higher intensity (n = 25 for tonic firing neurons in lobule III-V, n = 13 for tonic firing neurons in lobule X and n = 15 for gap firing neurons in lobule X). $^{*}P < 0.05$, both between tonic firing neurons in lobule III-V and tonic firing neurons in lobule X and between tonic firing neurons in lobule III-V and gap firing neurons in lobule X.

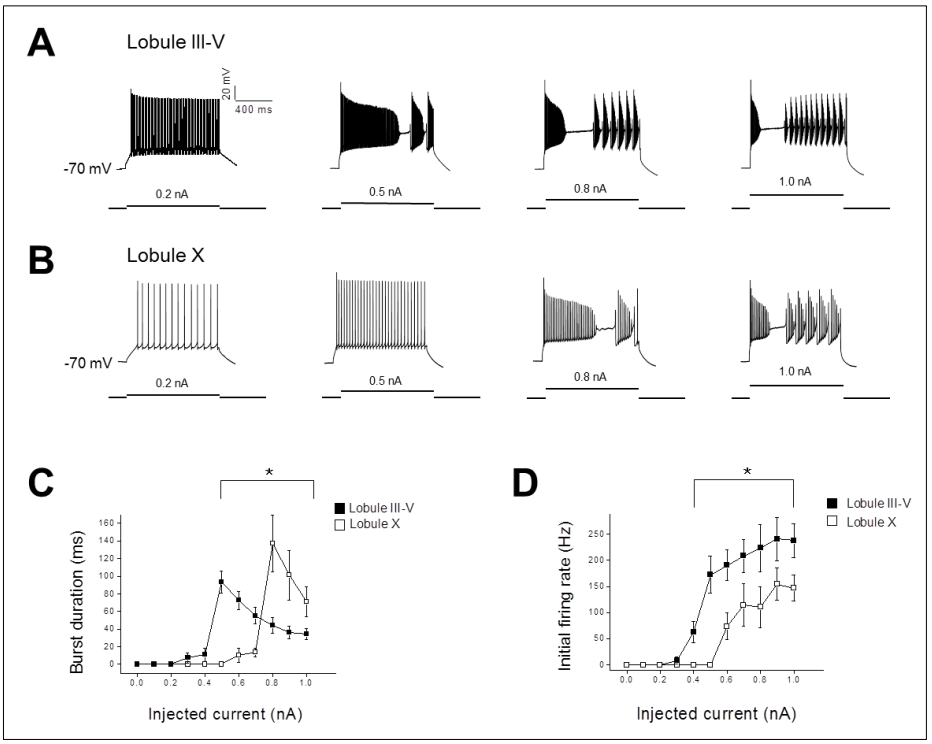

Figure 1-10. Comparison of electro-responsiveness of complex bursting neurons in lobule III-V and lobule X

Representative voltage responses evoked in complex bursting neurons of lobule III-V (**A**) and lobule X (**B**) by depolarizing current pulses of increasing amplitude (left to right). Neurons in lobule III-V showed Ca^{2+}-Na^{+} bursts at lower depolarizing current injection than neurons in lobule X. (**C**) Summary plot showing average burst duration vs. injected current in complex bursting neurons in lobule III-V (**A**) and lobule X (**B**). Average burst duration was increased in response to higher depolarizing current injection within low-intensity range, and then decreased with injection of highly depolarizing current. (**D**) Collected results displaying average initial firing rate vs. injected current. Higher initial firing rate was obtained with the injection of higher-intensity current (n = 12 for complex bursting neurons in lobule III-V, n = 7 for complex bursting neurons in lobule X). $^{*}P < 0.05$, between neurons in lobule III-V and lobule X.

DISCUSSION

Characterization of membrane properties of PCs is important in understanding how sensory information is processed and integrated lobule-specifically. This study showed that intrinsic membrane properties vary widely between PCs in lobule III-V and X.

Lobule-specific differences in membrane properties of PCs

Firing patterns. Four firing patterns were identified in PCs from acute slices. Previous studies have observed only tonic firing and complex bursting patterns in PCs from acute slices (15, 16), and these patterns were also observed in PCs of both lobule III-V and X in our study. Besides these firing patterns, initial bursting and gap firing patterns were observed in lobule X PCs, which had never been reported in acute slice preparation. The electrical activity of single PCs in the frog vestibulocerebellum in response to horizontal angular acceleration was reported (37). Four main classes of PCs were clearly categorized according to their general properties of responses to this form of physiological stimulation. These results were consistent with our findings that four distinct firing patterns of PCs were observed in the rat vestibulocerebellum (Figure 1-2), even though functional correlations between *in vitro* observation and *in vivo* responses need further investigation.

In tonic firing neurons, it is known that stimulus intensity of afferent input can be linearly transduced into spike frequency, which is suited to encode both the intensity and the duration of afferent excitation (38, 39). In complex bursting

neurons, it has been proposed that repetitive burst firing may be generated by rhythmic interactions between Ca^{2+} conductances and the hyperpolarizing conductances (18). The P/Q-type Ca^{2+} channels predominantly contribute to voltage-activated Ca^{2+} current at the age (P21-23) of rats which were used in this study (40), and have been reported to be responsible for the generation of Ca^{2+} spike which terminates each Ca^{2+}-Na^{+} burst (17, 41).

The ionic mechanism underlying the initial bursting pattern has been studied in other neurons in the CNS (26-28). Generation of initial bursting could be a result of either cumulative inactivation of Na^{+} current or activation of very strong outward K^{+} current at steady-state. From our results, we could find that one or more 4-AP sensitive K^{+} conductances may contribute to the formation of initial bursting pattern. These observations are consistent with the existence of 4-AP sensitive currents which have been shown to be possibly responsible for the initial bursting in neurons of mammalian cochlear nucleus or medial nucleus of the trapezoid body and avian nucleus magnocellularis (26-28). However, without voltage-clamp data, we could not rule out the contribution of multiple 4-AP sensitive K^{+} conductances, and estimate the magnitude of them. Rapid inactivation of fast Na^{+} current might also be partly responsible for the generation of initial bursting pattern since spike height and rate of rise were decreasing, and spike threshold was increasing in the successive spikes of initial burst. Moreover, additional current injection during the maintained current pulse did not evoke another spike. A single AP can inactivate sodium channels by more than 90% (42), so rapid recovery from the inactivation is essential to restore an availability of sodium channels to generate subsequent

spikes. In Nav1.6 knockout mice, transient Na^+ current is inactivated more rapidly than the wild type and resurgent sodium current is reduced by 90% (42, 43), and many of PCs could not maintain firing during current injections displaying initial bursting pattern. The reason for this was suggested that the reduction in resurgent current which leads to rapid recovery of Na^+ channels during repolarization, limited recovery of sodium channels, thus initiating depolarization block (44). Initial bursting neurons are unable to encode stimulus intensity through firing frequency, but may act as novelty detectors by discharging only at the onset of the afferent excitation. These neurons are well suited for encoding onset of stimulus. They are known to be best activated by steeply rising stimuli and capable of following high stimulation frequencies. For these reasons, they have been labeled as ‘high-pass filters’ or ‘coincidence detectors’ (35, 38, 39, 45).

Gap firing neurons have been identified in certain types of neurons in the CNS, and slow I_A which is activated at the subthreshold range of AP generation has been reported to be responsible for the gap firing pattern (22, 46). The presence of fast I_A has been reported in PCs (23, 47, 48), and the formation of gap firing pattern might be contributed by slow I_A in lobule X PCs. I_A has been shown to play an important role in synaptic integration by influencing subthreshold membrane properties, and could be involved in filtering subthreshold excitatory inputs by dampening synaptic excitatory signals in dendrites (49). Neurons with gap firing pattern are capable of firing repetitively over a range of stimulus intensities, thus may have voltage-dependent encoding properties. This type of neuron is known to be best

activated by slowly rising stimuli. When they are stimulated by high frequency stimuli with short duration, they integrate these stimuli over time. Thus, they have been named as ‘low-pass filters’ or ‘integrators’ (35, 38, 39, 45)

Active properties in response to depolarizing current injections. PCs in lobule X showed significantly lower AP amplitude and upstroke velocity, and higher AP threshold compared to lobule III-V, which might reflect decreased Na^+ channel activity in lobule X PCs. These results might be considered as a result of lobule-specific differences in the density of Na^+ channel expression or level of regulation of Na^+ channel activity by auxiliary β-subunits and kinases. Similar changes in parameters of AP waveform were observed in $Nav1.6^{-/-}$ mutant PCs (50). Among PCs in lobule X, gap firing neurons displayed much higher AP threshold and lower maximum rate of rise, which may be explained by the considerable inactivation of Na^+ channels during a slow ramp depolarization before the presence of first AP in response to current injections.

Tonic firing and complex bursting neurons in lobule X displayed lower firing rate compared with lobule III-V neurons. The frequency of Na^+ spike discharge may determine the intensity coding properties of neurons. In PCs, Na^+ spike frequency regulates the characteristics of the postsynaptic responses in DCN neurons (51, 52). The density of Na^+ current is very important in determining neuronal excitability. Spontaneous APs in PCs have been reported to be initiated perisomatically, and a reduction in perisomatic Na^+

channel availability by focal application of subsaturating concentration of tetrodotoxin resulted in increased AP threshold and decreased slope of AP upstroke (53). Reduced Na^+ channel availability also decreased frequency of AP firing, which was consistent with the modeling studies of isolated PCs demonstrating significant dependence of Na^+ spike firing rate on the density of transient Na^+ current (44). PCs express two isoforms of sodium channel α subunit; Nav1.1 channels which are localized in the soma and apical dendrites of PCs, and Nav1.6 channels which are distributed in cell bodies, dendrites, and axon initial segment (54). PCs of mice lacking Nav1.1 or Nav1.6 expression exhibited slower rates of evoked firing than those of wild type no matter how high intensity the current was injected (16, 44). In general, K+ channel activity is known to determine AP frequency and the shape of a neuron, have a role in setting the resting membrane potential, and control the strength of synaptic contacts between neurons (20, 21). The K^+ conductance which contributes to the control of postsynaptic excitability is predominantly mediated by voltage-gated channels from families Kv1-Kv4. Kv1 channels are known to suppress excitability, and have been reported to be critical for maintaining low frequency of Na^+ spikes and optimizing the timing of neuronal outputs in PCs (52). Kv3 channels have high activation threshold and fast activation/deactivation kinetics, and support high-frequency firing (34). Firing rate was shown to be substantially reduced in Kv3.3 knock-out PCs (55). Kv4 channels which are activated at subthreshold potentials are known to regulate postsynaptic membrane excitability by filtering subthreshold excitatory inputs. Ether-a-go-go related gene channels of which

inactivation rates vastly exceed activation rates, are expressed in PCs, and blocking of these channels lead to increase in firng rate in PCs (56). Most of voltage-gated K^+ channels except Kv3seem to exert their actions towards lowering neuronal excitability when activated. Along with the fact that PCs in lobule X possess lower input resistance and higher membrane capacitance compared to lobule III-V neurons, PCs in lobule X may have higher resting K^+ conductance which is mediated mainly by K^+ channels with relatively low activation threshold. Decreased firing rate of PCs in lobule X is likely to implement considerable downstream consequences in target neurons in the vestibular nuclei and DCN by diminishing frequency of inhibitory GABAergic projections. Further investigation of lobule-specific differences in the expressional density of Na^+ channel and its isoforms, and their roles in characterizing electrical activity will be crucial in understanding the functions of PCs with distinct firing patterns in cerebellar circuitry.

Significance of lobule-specific differences of membrane properties in signal processing

A substantial amount of sensory information enters into the cerebellar vermis, and different lobules (lobule III-V *vs.* X) receive different kinds of afferent information. The termination of a mossy fiber system usually restricted to a particular combination of lobules or folia. This characteristic distribution of mossy fiber systems has been used to subdivide the cerebellum into functional regions, such as vestibular, spinal, visual, and cerebropontine territories (57). The spinocerebellar mossy fibers including both ventral and dorsal tracts are

mainly distributed in lobule III-V (58). Both primary and secondary vestibulocerebellar fibers terminate in lobule X, ventral lobule IX, cortex in the depth of the vermal fissures, and to a lesser amount in lobules I-II (57, 59). Lobule X makes up a major part of vestibulocerebellum. It encodes vestibular information, and contributes to adaptive control of vestibular functions which are fundamental for survival by maintaining body equilibrium in the gravitational field. Cerebellar granule cells which receive synaptic input via mossy fibers and send signals to PCs via parallel fibers, have been reported to show distinct synaptic responses to specific types of sensory stimulation in region-specific manner (60). These findings indicate that signals from granule cells are carried to PCs distinctively according to their regions, which may be implicated in achieving lobule-specific signal processing. PCs in lobule X exhibited more diverse firing patterns than lobule III-V, and those characteristic patterns of output spike were distinct as a result of how each cell type processes its input. These results may reflect differences in the input-output functions of PCs according to their location in the cerebellar vermis since neurons with different firing patterns exhibit distinct stimulus-response properties in signal processing. This diversity of firing patterns observed in lobule X PCs might be thought to be well suited for signal processing of wide-range vestibular inputs with diverse characteristics.

Our study showed that PCs in lobule X probably possess lower excitability than lobule III-V neurons. Higher threshold and slower rate of rise of AP in lobule X PCs make neurons respond to stimuli less sensitively, and reduced firing rate diminishes the frequency of IPSC in target neuron in DCN and

vestibular nuclei. Consequently, when considering the functional circuitry of a coordinate system, adaptive control which is mediated by inhibitory projections of PCs, is less intensely modulated in response to the same intensity of stimuli in lobule X in comparison to lobule III-V. The lack of occurrence of Na^+ spike failure until rather higher intensity current injection in lobule X PCs possibly make themselves be more suitable for encoding wide range of both the intensity and the duration of afferent excitation than lobule III-V PCs. Furthermore, PCs in lobule X exhibited wide dynamic range in their input-output curve, and did not saturate their firing rates as readily as PCs in lobule III-V (Figure 1-9). This feature, in line with the previous findings about the linearity of transformation of synaptic input in the vestibular circuit (61), may be an important attribute of the PCs in vestibulocerebellum from the perspective of vestibular function in that vestibular system provides a remarkable linearity of vestibular reflexes.

In conclusion, PCs in lobule X, a part of vestibulocerebellum, present more heterogeneity in firing pattern, and in general exhibit lower excitability which may be due to decreased sodium channel activity compared to PCs in lobule III-V. However, the differences in signal processing properties will not be fully appreciated until we understand the interconnectivity of neurons and characterize input evoked by specific vestibular stimulation.

CHAPTER 2

Reduced spike frequency adaptation in Purkinje cells of the vestibulocerebellum

INTRODUCTION

Purkinje cells (PCs) are the only output neurons from the cerebellar cortex, and the information into the cerebellum converges in the extensive dendritic arbors of PCs. This information is encoded into a new signal by PCs, which is delivered to deep cerebellar nucleus (DCN) or vestibular nucleus (VN) via GABAergic axonal projections of PCs. PCs show spontaneous firing of action potentials (APs) both in *in vitro* preparation where synaptic inputs have been blocked (2) and in *in vivo* condition where spontaneous inhibitory synaptic activities into PCs are present (3).

Cerebellar vermis consists of ten lobules (lobule I to X). Among them, lobules III, IV, and V are known as spinocerebellum because they receive major afferent input through ventral spinocerebellar tract (7), and lobule X is considered as a part of vestibulocerebellum since it receives extensive vestibular input via primary and secondary vestibular afferent (8, 62). It is conceivable that PCs in different lobules may have different input-output function as each lobule is considered to encode different kinds of sensory information. In the previous study we reported that intrinsic membrane properties vary widely between PCs in lobule III-V and X in a way that PCs in lobule X are less excitable, possess more diversity in firing pattern, and show wider dynamic range (63).

Spike frequency adaptation (SFA) is defined as a decrease in instantaneous firing rate during a sustained current injection. In vestibular nucleus, neurons exhibit a diversity of membrane properties including different extent of SFA (64, 65). SFA has been considered to play an important role in the processing of sensory stimuli. Neurons can be protected from excitotoxicity by the saturation of firing rate, and sensory responses can be tuned to specific features of stimuli by SFA. SFA can also emphasize changes in stimulus parameters (66-68). PCs also have been reported to exhibit SFA of varying degrees (56). However, little is known about the lobule-specific difference in

the degree of SFA in PCs. In the present study, we compared the SFA of cerebellar PCs between lobule III-V and X to investigate if afferent stimulation is encoded in a lobule-specific way by different degree of SFA. We found that the degree of SFA was different between PCs in lobule X and lobule III-V, which may render PCs in different lobules lobule-specificly tuned for firing dynamics.

MATERIALS AND METHODS

1. Slice preparation

Parasagittal slices of the cerebellar vermis (300 μm thick) were prepared from P21−P23 Sprague-Dawley rats using a vibratome (Microm HM 650V, Germany). The slices were taken from approximately 500 μm to both sides of the midline in the ice-cold standard artificial cerebrospinal fluid (ACSF) containing (in mM): 124 NaCl, 2.5 KCl, 1 Na_2HPO_4, 1.3 $MgCl_2$, 2.5 $CaCl_2$, 26.2 $NaHCO_3$, and 20 D-glucose, bubbled with 95% O_2 and 5% CO_2. After cutting, slices were kept for 30min at 35° C and then for up to 8hr at 25° C in ACSF.

2. Whole cell patch-clamp recordings

Somatic whole-cell current-clamp recordings were obtained from PCs in lobule III-V and lobule X as described previously (63). 100 μM picrotoxin (Sigma, St. Louis, MO, USA) and 1mM kynurenic acid (Sigma, St. Louis, MO, USA) were added to the perfusate. The series resistance was usually between 11 and 15 MΩ. All data were recorded using an EPC-9 patch-clamp amplifier (HEKA Elektronik, Germany), and the signals were filtered at 2 kHz. Glass pipettes (2−4 MΩ) were filled with internal solution containing (in mM): K gluconate 135, NaCl 7, MgATP 2, NaGTP 0.3, HEPES 10, EGTA 0.5, phosphocreatine di(tris) salt 10, pH 7.2. Recordings were performed at 30° C. Recordings were started 5 min after obtaining the whole-cell configuration to allow diffusion of the internal solution into the cytosol.

3. Data measurement and analysis

Data were acquired by Pulse software (HEKA Elektronik, Germany) and analyzed offline with the program IgorPro (Wavemetrics, Lake Oswego, OR, USA). Neuronal responses were studied at membrane potential of -70 mV to minimize the influence of voltage dependent changes on membrane conductance. Neurons in which the holding current was greater than 400 pA were discarded from analysis. Hyperpolarizing and depolarizing current injections (from -600 pA to +1000 pA with increments of 100 pA) of 1 s duration were applied with a step interval of 5 s to classify firing pattern of PCs, and each series was repeated for three trials. The voltage threshold was determined from the first AP at 'low-frequency firing' by measuring the membrane potential at which d*V*/d*t* first entered within the range 30–60 mV/ms (63). AP amplitude was measured from a baseline set at threshold, and AP duration was measured as half-width of AP. The amplitude of single spike afterhyperpolarization (AHP) was measured as the difference between the AP threshold and the negative peak of fast AHP (fAHP) or slow AHP (sAHP) (Figure 2-3) (63). The coefficient of variation (CV) of interspike intervals (ISIs) was presented as the percentage (%) by multiplying the ratio of the standard deviation to the mean value of ISIs by 100. Data are expressed as mean±SEM and '*n*' indicates the number of neurons tested. Statistical evaluations were performed using *t*-test or one-way ANOVA with *post hoc* Scheffe's test. $P<0.05$ was considered to be significant.

RESULTS

PCs showing tonic firing or gap firing patterns which are capable of repetitive firing over a range of stimulus intensities (63) are included in this study. Tonic firing neurons (TFNs) are characterized by continued discharge of APs in response to depolarizing current commands, and gap firing neurons (GFN) have a characteristic delay between the onset of the current injection and the first AP (63).

Comparison of ISI and CV between PCs from lobule III-V and X

The duration and shape of spike AHP which is known to have a crucial influence on ISI or SFA are highly dependent on the neuron's firing state. So, we examined the extent of SFA in two different firing conditions: 'low-frequency firing (LFF)' and 'high-frequency firing (HFF)' (Figure 2-1). To elicit 'LFF', low-intensity depolarizing current injection which was defined as the minimum current magnitude required to elicit about 20 spikes (15-25 spikes) during 1s of injection current steps in 5 pA increments to mimic the *in vitro* condition of spontaneous firing (Figure 2-1, second column). Under our experimental settings, PCs tend to show a sustained firing without any current injection (n=52, data not shown), and the spontaneous firing rate was 20±1.5 (14-27) Hz which was similar with that of a previous study (69). The depolarizing current injection to elicit 'LFF' was significantly lower in TFNs in lobule III-V (152.1±18.7 pA, n=28) than TFNs in lobule X (321.5±13.6 pA, n=85) or GFNs in lobule X (326.4±13.9 pA, n=46) (P<0.05). Number of spikes was 20.3±1.2 (n=28) for TFNs in lobule III-V, 21.6±0.5 (n=85), and 20.9±0.6 (n = 46) for TFNs and GFNs in lobule X, respectively. Some PCs did not fire at low rates even at the stimulus level around the rheobase to skip the 'LFF' range (15-25 Hz), and these neurons were discarded from the

evaluations (9 out of 37 TFNs in lobule III-V, 6 out of 91 TFNs, and 4 out of 50 GFNs in lobule X). To elicit 'HFF', high-intensity depolarizing current was injected, which was defined as the highest depolarizing current at which PC showed sustained firing throughout the current step (1 s) without Na^+ spike failure (Figure 2-1, third column). The depolarizing current injection to elicit 'HFF' was significantly lower in TFNs in lobule III-V (610.7±43.1 pA, *n*=37) than TFNs or GFNs in lobule X (815.8±28.9 pA, *n*=91; 810.0±44.1 pA, *n*=50). Number of spikes during 1s of 'HFF' was 90.6±5.4 (*n*=37) for TFNs in lobule III-V, 54.8±3.5 (*n*=91), and 62.7±4.1 (*n*=50) for TFNs and GFNs in lobule X, respectively. As shown in the previous study (63), PCs in lobule III-V required lower depolarizing current injection to elicit LFF or HFF, and showed larger number of spikes in HFF compared with those in lobule X.

ISIs normalized by the first ISI were plotted against the progression of spikes. In low-frequency spike trains, TFNs in lobule III-V (*n*=28) showed gradual lengthening of ISI due to SFA (Figure 2-2A). In TFNs (*n*=85) and GFNs (*n*=46) in lobule X, normalized ISIs stayed around 1 during firing, which means that these neurons exhibit lack of SFA (Figure 2-2A). In 'HFF', TFNs in lobule III-V (*n*=37) exhibited gradual, but low degree of SFA (Figure 2-2B). In TFNs (*n*=91) and GFNs (*n*=50) in lobule X, ISI increased dramatically during the first four spikes and showed little change after that (Fig. 2B). The ratio of the tenth (ISI_{10}) and the last (ISI_{last}) ISIs to the first ISI (ISI_{10}/ ISI_1 and ISI_{last}/ ISI_1) were significantly different from each other in TFNs in lobule III-V with both 'LFF' (ISI_{10}/ISI_1=1.92±0.09 and ISI_{last}/ISI_1=2.80±0.18, **P*<0.05) and 'HFF' (ISI_{10}/ISI_1 = 1.43±0.04 and ISI_{last}/ISI_1 = 1.69±0.05, ***P*<0.05) (Figure 2-2C). In contrast, comparisons of ISI_{10}/ISI_1 with ISI_{last}/ISI_1 were not significantly different in TFNs (1.27±0.05 and 1.26±0.06 with 'LFF'; 2.41±0.08 and 2.43±0.09 with 'HFF') and GFNs (1.05±0.03 and 1.00±0.04 with 'LFF'; '2.32±0.09' and '2.37±0.13' with 'HFF') in lobule X (Figure 2-

2C). ISI_{10}/ISI_1 in 'LFF' was significantly higher in TFNs in lobule III-V than neurons in lobule X (***P<0.05). These results indicate that TFNs in lobule III-V exhibit higher degree of SFA than neurons in lobule X especially in 'LFF'.

Regularity of ISI was evaluated by measuring CV of ISI (Figure 2-2D). TFNs in lobule III-V showed significantly higher CV in 'LFF' than 'HFF' (26.1±2.8% *vs.* 9.6±0.6%, $^{\ddagger}P$<0.05). CVs of TFNs (8.9±0.5%) and GFNs (8.0±0.4%) in lobule X were significantly lower than that of TFNs in lobule III-V (26.1±2.8 %) in 'LFF' ($^{\dagger}P$<0.05). In 'HFF', CVs were not significantly different among TFNs in lobule III-V, TFNs and GFNs in lobule X (9.6±0.6%, 8.7±0.3%, and 8.4±0.5%, respectively). However, we cannot rule out the possibility that much steeper increase in ISI during the first four spikes in lobule X neurons may diminish the degree of regularity, even though the regularity of ISI after the fourth spike is more prominent in those neurons.

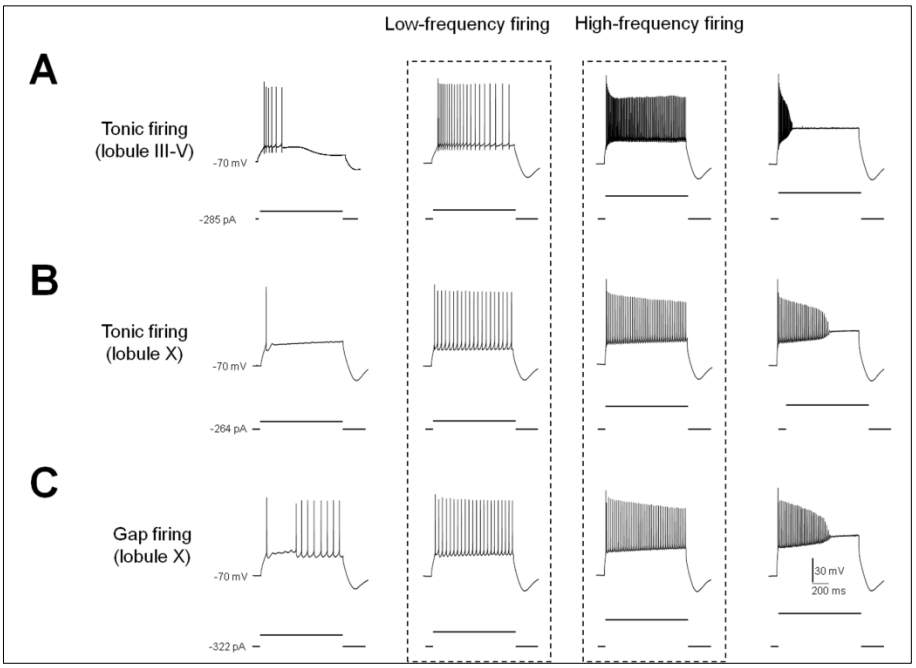

Figure 2-1. Representative firing patterns of tonic firing in lobule III-V (A, *n*=37), tonic (B, *n*=91) and gap firing (C, *n*=50) in lobule X of cerebellar vermis.

'Low-frequency firing' (dotted outline in the second column), and 'High-frequency firing' (dotted outline in the third column) were elicited. Note that the failure of Na^+ spike is observed in the fourth column.

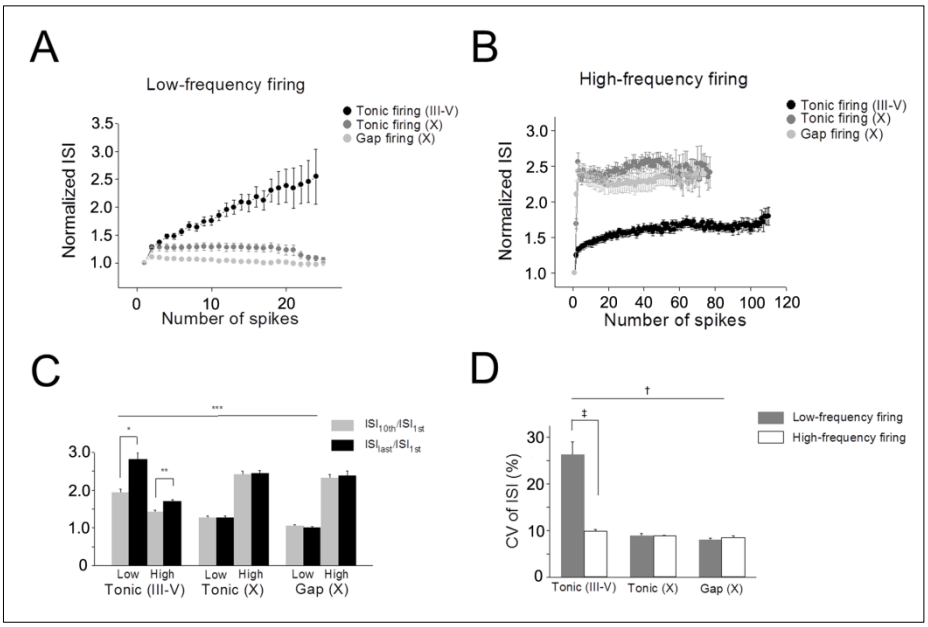

Figure 2-2. Comparisons of interspike intervals (ISIs) among neurons exhibiting tonic or gap firing pattern in lobule III-V and X.

(**A**) Plot of ISI normalized by first ISI vs. number of spikes in 'LFF' traces. SFA was more prominent in lobule III-V PCs, compared with lobule X PCs. (**B**) Plot of ISI normalized by first ISI vs. number of spikes in 'HFF' traces. (**C**) Summary data comparing SFA for neurons in lobule III-V and X. ISI_{last}/ISI_{1st} was significantly higher than ISI_{10th}/ISI_{1st} in lobule III-V neurons both in 'LFF' and 'HFF' (*P<0.05, **P<0.05). Respective comparisons of ISI_{10th}/ISI_{1st} or ISI_{last}/ISI_{1st} between TFNs in lobule III-V and TFNs or GFNs in lobule X in LFF exhibited significant difference (***P<0.05). (**D**) Comparison of coefficient of variation (CV) of ISIs among neurons exhibiting tonic or gap firing pattern in lobule III-V and X. Tonic firing neurons in lobule III-V showed significantly higher CV of ISI in 'LFF' than 'HFF' (†P<0.05). In

'LFF', CV of ISI was 26.1±2.8 % for tonic firing neurons in lobule III-V, 8.9±0.5% for tonic firing neurons in lobule X, and 8.0±0.4% for gap firing neurons in lobule X, which showed significant difference ($^{\ddagger}P<0.05$). Whereas, there was no significant difference in CV of ISI among neurons in lobule III-V and lobule X when 'HFF' was elicited.

Comparison of ISI and CV according to the shape of AHP in lobule X PCs

The morphology of AHP has been shown to correlate with spike regularity or the extent of SFA (64, 70). In lobule X, both the monophasic AHP which has only a fast component (fAHP) and the triphasic AHP which has an initial hyperpolarization followed by a depolarization and then a slow component (sAHP) were observed in PCs, whereas only monophasic AHP was observed in lobule III-V PCs. To investigate the influence of AHP shape on SFA or firing regularity, we classified lobule X PCs into 3 subgroups according to the ratio of sAHP to fAHP (sAHP/fAHP=0, 0<sAHP/fAHP<1 and sAHP/fAHP≥1) (Figure 2-3). There were no significant differences of ISI_{10}/ISI_1 or ISI_{last}/ISI_1 among 3 subgroups both in 'LFF' and 'HFF' (P>0.05, Figure 2-3D). CVs of ISI were not also significantly different among subgroups both in 'LFF' and 'HFF' (P>0.05, Fig. 3E). These results indicate that SFA is not much influenced by the morphology of AHP in lobule X PCs.

We examined if AP duration is changed during firing (Figure 2-4A-C), since AP duration has been reported to be prolonged during spike train in adapting neurons (70). In the present study, there was no significant difference between normalized (by first AP) 10th and last AP duration in PCs of lobule III-V and lobule X in 'LFF' (Figure 2-4D), even though the extent of SFA was significantly different between PCs in lobule III-V and X (Figure 2-2A and C). No significant difference was also observed between normalized (by first AP) 10th and last AP duration in 'HFF' (Figure 2-4E). Previous study noted that AP duration is increased during repetitive spiking in adapting neurons, but not in nonadapting neurons in the neocortex (70), but our data showed that the

extent of SFA was not significantly related to the change of AP duration in PCs.

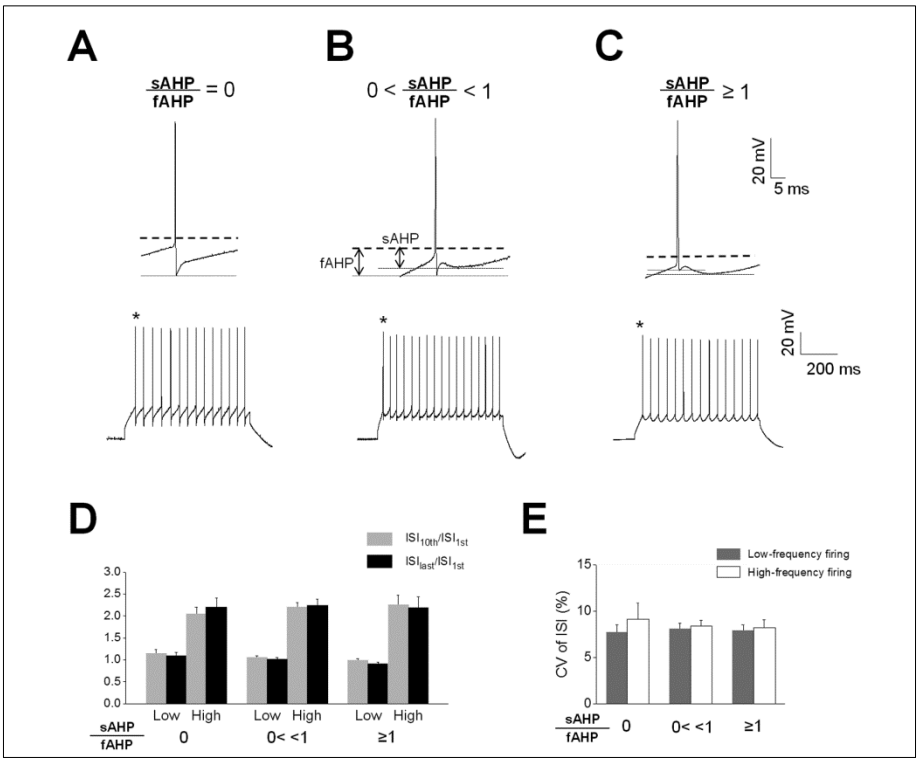

Figure 2-3. Shape of afterhyperpolarization (AHP) of single spike in lobule X neurons.

The triphasic appearance of AHP with an initial fast AHP (fAHP) followed by a depolarizing phase and then slow AHP (sAHP) was observed in tonic and gap firing neurons in lobule X (see **B** and **C**). The ratio of the amplitude of sAHP to fAHP in the 5th spike (*) of 'LFF' was classified into 3 groups; sAHP/fAHP=0 (**A**), 0<sAHP/fAHP<1 (**B**), and sAHP/fAHP≥1 (**C**). See magnified 5th AP on lower panels of A, B, and C. (**D**) Respective comparison of ISI_{10th}/ISI_{1st} or ISI_{last}/ISI_{1st} among sAHP/fAHP=0 group (1.14±0.09 or 1.09±0.08 in 'LFF' and 2.04±0.16 or 2.19±0.22 in 'HFF'), 0<sAHP/fAHP<1 group (1.05±0.04 or 1.01±0.04 in 'LFF' and 2.20±0.11 or

2.24±0.15 in ‘HFF’), and sAHP/fAHP≥1 group (0.99±0.04 or 0.91±0.04 in ‘LFF’ and 2.25±0.22 or 2.19±0.25 in ‘HFF’) showed no significant difference in both ‘LFF’ and ‘HFF’ neurons. E: Comparison of CV of ISI among 3 groups showed no significant difference in both ‘LFF’ and ‘HFF’ neurons.

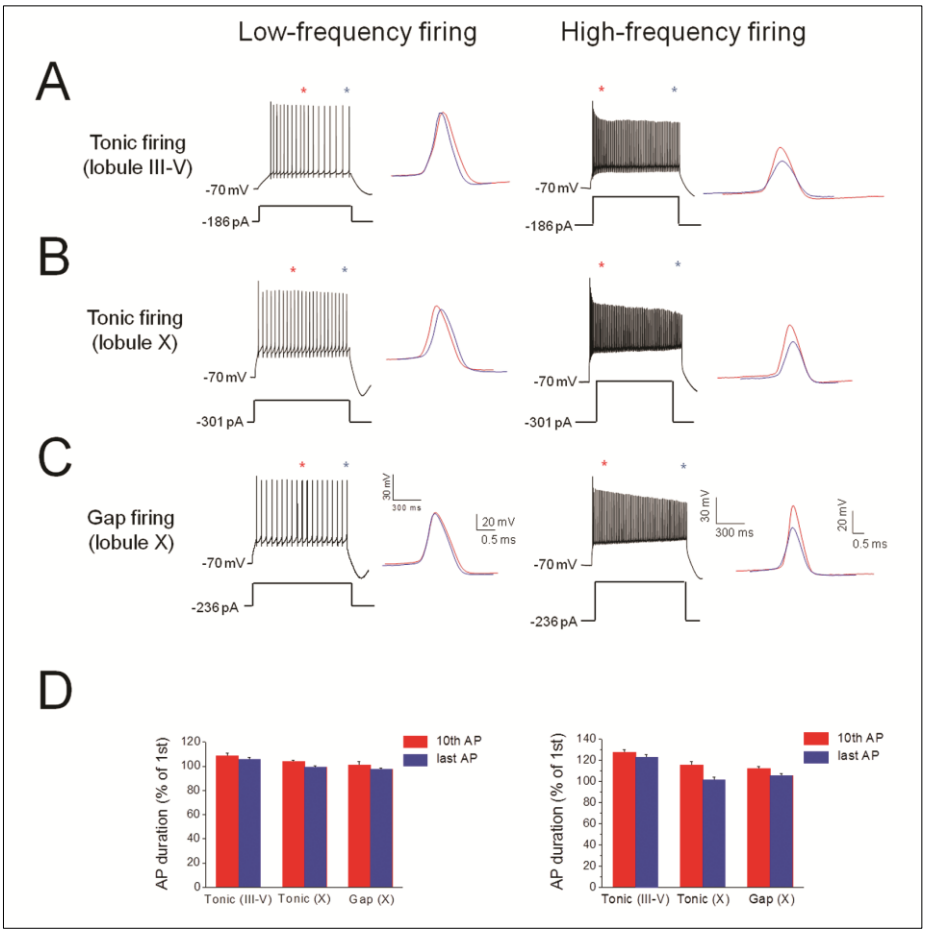

Figure 2-4. Changes of duration of single action potentials (APs) in 'low-frequency firing' and 'high-frequency firing'.

Representative traces of tonic firing neurons in lobule III-V (**A**), tonic firing (**B**), and gap firing (**C**) in lobule X. 'Low-frequency firing' and 'high-frequency firing' of the same neurons are displayed in left and right column, respectively. The red and blue dots in the traces indicate the 10th and last spikes, respectively. The superimposed traces of the 10th (red) and last (blue) spikes in 'low-frequency firing' and 'high-frequency firing' from tonic firing in lobule III-V (**A**), tonic firing (**B**), and gap firing (**C**) in lobule X are also displayed. **D** and **E**: Comparison of the effect of repetitive firing on the

duration of AP in ‘low-frequency firing’ (**D**) and ‘high-frequency firing’ (**E**). The duration of the 10th and the last AP (as a percentage of the first AP) is depicted as red and blue bar, respectively. Respective comparisons of the duration (% of the first AP) of the 10th or the last AP in ‘low-frequency firing’ were not significantly different among tonic firing in lobule III-V (108.8±2.2 or 105.8±1.7), tonic firing in lobule X (103.6±1.6 or 98.9±1.7) and gap firing in lobule X (101.2±2.7 or 97.2±1.5) (**D**). In ‘high-frequency firing’, AP duration (% of the first AP) of both 10th and the last AP did not show significant difference in tonic firing neurons in lobule III-V (10th, 127.5±2.4%; last, 122.2±3.0%; n=28), tonic (10th, 115.2±3.6%; last, 101.2±2.5%; n=85) or gap firing neurons (10th, 111.7±2.3%; last, 105.0±2.3%; n=46) in lobule X (**E**).

DISCUSSION

In the present study, we showed the differences in the degree of SFA and discharge regularity between PCs in lobule X (vestibulocerebellum) and lobule III-V (spinocerebellum) during firing. These differences are more prominent when neurons are firing in low-frequency (~20 spikes/s).

SFA is a striking feature of neural dynamics and a widespread phenomenon in spiking neurons. Although SFA is observed in most of firing neurons, little or no SFA has been reported in some neurons such as fast-spiking neocortical GABAergic neurons (71) as observed in PCs of lobule X in this study. Ionic currents which have been demonstrated to contribute to SFA include slow recovery from inactivation of the fast Na^+ current, M-type K^+ current (72), Ca^{2+}-sensitive K^+ current (73), Ca^{2+}-sensitive Cl^- current (74), and Na^+-sensitive K^+ currents (75). From computational simulation, SFA was proposed as means for high-pass filtering to select rapid over slow transients (76, 77). Another proposed role for SFA is dynamic range modulation which is important in early sensory processing by shifting tuning curves (66, 77).

SFA or the regularity of spike timing has been an important issue in understanding vestibular system, and firing regularity was mainly investigated in the primary and secondary vestibular afferents. Mammalian primary vestibular nerve comprises highly regular and highly irregular population, and they may compensate for differences in the dynamic loads of various reflexes or of individual reflexes in different parts of their frequency range (to see review, (78)). Regularly and irregularly firing VN neurons may participate in different frequency-tuned networks controlling gaze and posture (79). CV of ISI of VN neurons has been reported to be related to AHP profiles which are significantly influenced by apamin-sensitive K^+ current (64). As shown in the previous studies (15, 80), SFA observed in PCs of lobule III-V may be related to apamin-sensitive K^+ current. However, lobule X PCs with different AHP profiles did not exhibit differences in the degree of SFA and firing regularity

in the present study (Figure 2-3). Moreover, the degree of SFA was not related to the change of AP duration during the repetitive firing (Figure 2-4). Thus, the mechanisms which are responsible for the interlobular difference of the degree of SFA may be different from those which have been reported to underlie the generation of SFA.

Primary vestibular afferents and VN consist of neurons with both regular and irregular firing, whereas vestibulocerebellum (lobule X), as a coordinator in the vestibular circuitry, is composed of PCs with less degree of SFA and more regular firing in general especially when PCs are firing in low-frequency. The vestibular system provides a remarkable linearity of vestibular reflexes exhibiting linearity of transformation of synaptic input in the vestibular circuit especially at the level of the connection between the afferent input and the secondary vestibular neurons (61), which contributes to the high-fidelity signal processing of vestibular input. In the present study, lobule X PCs showed differential features in SFA according to the state of firing frequency. In 'LFF', lobule X PCs discharge spikes more regularly with less degree of SFA compared with lobule III-V, which may suggest that the adaptive control of vestibular system which is mediated by inhibitory projection of vestibulocerebellar PCs, is more tonically but less intensely modulated during the low-intensity vestibular stimulation or even during without the vestibular stimulation (Figure 2-2A). On the other hand, in 'HFF', the CVs of ISI were not significantly different between PCs in lobule X and lobule III-V (Figure 2-2D), and ISI was rapidly increased during the first four spikes and then showed little change in lobule X (Figure 2-2B). When high-intensity vestibular stimulation is given, vestibulocerebellar PCs modulate vestibular system more intensely by firing with high-frequency at the beginning of stimulation (during the first several spikes) and then discharge tonically afterwards, thus they may possess different modes of response at the beginning and the steady state of the stimulation.

In conclusion, PCs in lobule X present higher firing regularity and less degree of SFA especially in response to low-intensity stimulus. However, the mechanisms which underlie the interlobular difference of SFA still remain to be elucidated. The functional consequences of the findings of this study would be more clearly interpreted if we understand the interconnectivity of neurons and characterize input evoked by specific vestibular stimulation.

REFERENCES

1. Strick PL, Dum RP, Fiez JA. Cerebellum and nonmotor function. Annu Rev Neurosci. 2009;32:413-34.
2. Hausser M, Clark BA. Tonic synaptic inhibition modulates neuronal output pattern and spatiotemporal synaptic integration. Neuron. 1997 Sep;19(3):665-78.
3. Armstrong DM, Rawson JA. Activity patterns of cerebellar cortical neurones and climbing fibre afferents in the awake cat. J Physiol. 1979 Apr;289:425-48.
4. Womack M, Khodakhah K. Active contribution of dendrites to the tonic and trimodal patterns of activity in cerebellar Purkinje neurons. J Neurosci. 2002 Dec 15;22(24):10603-12.
5. Womack MD, Khodakhah K. Somatic and dendritic small-conductance calcium-activated potassium channels regulate the output of cerebellar purkinje neurons. J Neurosci. 2003 Apr 1;23(7):2600-7.
6. McKay BE, Turner RW. Physiological and morphological development of the rat cerebellar Purkinje cell. J Physiol. 2005 Sep 15;567(Pt 3):829-50.
7. Larsell O, Jansen J. The comparative anatomy and histology of the cerebellum: The human cerebellum, cerebellar connections, and cerebellar cortex. Minneapolis: The University of Minnesota press; 1972.

8. Barmack NH, Baughman RW, Errico P, Shojaku H. Vestibular primary afferent projection to the cerebellum of the rabbit. J Comp Neurol. 1993 Jan 22;327(4):521-34.
9. Barmack NH, Baughman RW, Eckenstein FP. Cholinergic innervation of the cerebellum of the rat by secondary vestibular afferents. Ann N Y Acad Sci. 1992 May 22;656:566-79.
10. Wadiche JI, Jahr CE. Patterned expression of Purkinje cell glutamate transporters controls synaptic plasticity. Nat Neurosci. 2005 Oct;8(10):1329-34.
11. Kim YS, Shin JH, Hall FS, Linden DJ. Dopamine signaling is required for depolarization-induced slow current in cerebellar Purkinje cells. J Neurosci. 2009 Jul 1;29(26):8530-8.
12. Llinas R, Sugimori M. Electrophysiological properties of in vitro Purkinje cell somata in mammalian cerebellar slices. J Physiol. 1980 Aug;305:171-95.
13. Williams SR, Christensen SR, Stuart GJ, Hausser M. Membrane potential bistability is controlled by the hyperpolarization-activated current I(H) in rat cerebellar Purkinje neurons in vitro. J Physiol. 2002 Mar 1;539(Pt 2):469-83.
14. Zhu L, Scelfo B, Tempia F, Sacchetti B, Strata P. Membrane excitability and fear conditioning in cerebellar Purkinje cell. Neuroscience. 2006 Jul 7;140(3):801-10.

15. Edgerton JR, Reinhart PH. Distinct contributions of small and large conductance Ca2+-activated K+ channels to rat Purkinje neuron function. J Physiol. 2003 Apr 1;548(Pt 1):53-69.
16. Kalume F, Yu FH, Westenbroek RE, Scheuer T, Catterall WA. Reduced sodium current in Purkinje neurons from Nav1.1 mutant mice: implications for ataxia in severe myoclonic epilepsy in infancy. J Neurosci. 2007 Oct 10;27(41):11065-74.
17. Ovsepian SV, Friel DD. The leaner P/Q-type calcium channel mutation renders cerebellar Purkinje neurons hyper-excitable and eliminates Ca2+-Na+ spike bursts. Eur J Neurosci. 2008 Jan;27(1):93-103.
18. Pouille F, Cavelier P, Desplantez T, Beekenkamp H, Craig PJ, Beattie RE, et al. Dendro-somatic distribution of calcium-mediated electrogenesis in purkinje cells from rat cerebellar slice cultures. J Physiol. 2000 Sep 1;527 Pt 2:265-82.
19. Cavelier P, Beekenkamp H, Shin HS, Jun K, Bossu JL. Cerebellar slice cultures from mice lacking the P/Q calcium channel: electroresponsiveness of Purkinje cells. Neurosci Lett. 2002 Nov 15;333(1):64-8.
20. Hille B. Ionic Channels of Excitable Membranes, 2nd edition, Sinauer Press, Sunderland, MA. 1992.
21. Mathie A, Wooltorton JR, Watkins CS. Voltage-activated potassium channels in mammalian neurons and their block by novel pharmacological agents. General pharmacology. 1998 Jan;30(1):13-24.

22. Rudy B, Chow A, Lau D, Amarillo Y, Ozaita A, Saganich M, et al. Contributions of Kv3 channels to neuronal excitability. Ann N Y Acad Sci. 1999 Apr 30;868:304-43.
23. Wang D, Schreurs BG. Characteristics of IA currents in adult rabbit cerebellar Purkinje cells. Brain Res. 2006 Jun 22;1096(1):85-96.
24. Taglialatela M, Vandongen AM, Drewe JA, Joho RH, Brown AM, Kirsch GE. Patterns of internal and external tetraethylammonium block in four homologous K+ channels. Mol Pharmacol. 1991 Aug;40(2):299-307.
25. Ikeda SR, Korn SJ. Influence of permeating ions on potassium channel block by external tetraethylammonium. J Physiol. 1995 Jul 15;486 (Pt 2):267-72.
26. McElvain LE, Bagnall MW, Sakatos A, du Lac S. Bidirectional plasticity gated by hyperpolarization controls the gain of postsynaptic firing responses at central vestibular nerve synapses. Neuron. 2010 Nov 18;68(4):763-75.
27. van Welie I, du Lac S. Bidirectional control of BK channel open probability by CAMKII and PKC in medial vestibular nucleus neurons. J Neurophysiol. 2011 Apr;105(4):1651-9.
28. Banks MI, Smith PH. Intracellular recordings from neurobiotin-labeled cells in brain slices of the rat medial nucleus of the trapezoid body. J Neurosci. 1992 Jul;12(7):2819-37.

29. Crepel F, Penit-Soria J. Inward rectification and low threshold calcium conductance in rat cerebellar Purkinje cells. An in vitro study. J Physiol. 1986 Mar;372:1-23.

30. Armano S, Rossi P, Taglietti V, D'Angelo E. Long-term potentiation of intrinsic excitability at the mossy fiber-granule cell synapse of rat cerebellum. J Neurosci. 2000 Jul 15;20(14):5208-16.

31. Farley J, Richards WG, Ling LJ, Liman E, Alkon DL. Membrane changes in a single photoreceptor cause associative learning in Hermissenda. Science. 1983 Sep 16;221(4616):1201-3.

32. Roth A, Hausser M. Compartmental models of rat cerebellar Purkinje cells based on simultaneous somatic and dendritic patch-clamp recordings. J Physiol. 2001 Sep 1;535(Pt 2):445-72.

33. Pape HC. Queer current and pacemaker: the hyperpolarization-activated cation current in neurons. Annu Rev Physiol. 1996;58:299-327.

34. Raman IM, Bean BP. Ionic currents underlying spontaneous action potentials in isolated cerebellar Purkinje neurons. J Neurosci. 1999 Mar 1;19(5):1663-74.

35. Heinke B, Ruscheweyh R, Forsthuber L, Wunderbaldinger G, Sandkuhler J. Physiological, neurochemical and morphological properties of a subgroup of GABAergic spinal lamina II neurones identified by expression of green fluorescent protein in mice. J Physiol. 2004 Oct 1;560(Pt 1):249-66.

36. Llinas R, Sugimori M. Electrophysiological properties of in vitro Purkinje cell dendrites in mammalian cerebellar slices. J Physiol. 1980 Aug;305:197-213.

37. Nelson AB, Krispel CM, Sekirnjak C, du Lac S. Long-lasting increases in intrinsic excitability triggered by inhibition. Neuron. 2003 Oct 30;40(3):609-20.

38. Prescott SA, De Koninck Y. Four cell types with distinctive membrane properties and morphologies in lamina I of the spinal dorsal horn of the adult rat. J Physiol. 2002 Mar 15;539(Pt 3):817-36.

39. Ruscheweyh R, Sandkuhler J. Lamina-specific membrane and discharge properties of rat spinal dorsal horn neurones in vitro. J Physiol. 2002 May 15;541(Pt 1):231-44.

40. Meacham CA, White LD, Barone S, Jr., Shafer TJ. Ontogeny of voltage-sensitive calcium channel alpha(1A) and alpha(1E) subunit expression and synaptic function in rat central nervous system. Brain Res Dev Brain Res. 2003 Apr 14;142(1):47-65.

41. Mori Y, Wakamori M, Oda S, Fletcher CF, Sekiguchi N, Mori E, et al. Reduced voltage sensitivity of activation of P/Q-type Ca2+ channels is associated with the ataxic mouse mutation rolling Nagoya (tg(rol)). J Neurosci. 2000 Aug 1;20(15):5654-62.

42. Raman IM, Bean BP. Resurgent sodium current and action potential formation in dissociated cerebellar Purkinje neurons. J Neurosci. 1997 Jun 15;17(12):4517-26.

43. Kohrman DC, Smith MR, Goldin AL, Harris J, Meisler MH. A missense mutation in the sodium channel Scn8a is responsible for cerebellar ataxia in the mouse mutant jolting. J Neurosci. 1996 Oct 1;16(19):5993-9.

44. Khaliq ZM, Gouwens NW, Raman IM. The contribution of resurgent sodium current to high-frequency firing in Purkinje neurons: an experimental and modeling study. J Neurosci. 2003 Jun 15;23(12):4899-912.

45. Schneider SP. Spike frequency adaptation and signaling properties of identified neurons in rodent deep spinal dorsal horn. J Neurophysiol. 2003 Jul;90(1):245-58.

46. Kolkman KE, Moghadam SH, du Lac S. Intrinsic physiology of identified neurons in the prepositus hypoglossi and medial vestibular nuclei. J Vestib Res. 2011;21(1):33-47.

47. Sacco T, Tempia F. A-type potassium currents active at subthreshold potentials in mouse cerebellar Purkinje cells. J Physiol. 2002 Sep 1;543(Pt 2):505-20.

48. Wang Y, Strahlendorf JC, Strahlendorf HK. A transient voltage-dependent outward potassium current in mammalian cerebellar Purkinje cells. Brain Res. 1991 Dec 13;567(1):153-8.

49. Hoffman DA, Magee JC, Colbert CM, Johnston D. K+ channel regulation of signal propagation in dendrites of hippocampal pyramidal neurons. Nature. 1997 Jun 26;387(6636):869-75.

50. Swensen AM, Bean BP. Robustness of burst firing in dissociated purkinje neurons with acute or long-term reductions in sodium conductance. J Neurosci. 2005 Apr 6;25(14):3509-20.
51. Telgkamp P, Padgett DE, Ledoux VA, Woolley CS, Raman IM. Maintenance of high-frequency transmission at purkinje to cerebellar nuclear synapses by spillover from boutons with multiple release sites. Neuron. 2004 Jan 8;41(1):113-26.
52. McKay BE, Molineux ML, Mehaffey WH, Turner RW. Kv1 K+ channels control Purkinje cell output to facilitate postsynaptic rebound discharge in deep cerebellar neurons. J Neurosci. 2005 Feb 9;25(6):1481-92.
53. Khaliq ZM, Raman IM. Relative contributions of axonal and somatic Na channels to action potential initiation in cerebellar Purkinje neurons. J Neurosci. 2006 Feb 15;26(7):1935-44.
54. Schaller KL, Caldwell JH. Expression and distribution of voltage-gated sodium channels in the cerebellum. Cerebellum. 2003;2(1):2-9.
55. Akemann W, Knopfel T. Interaction of Kv3 potassium channels and resurgent sodium current influences the rate of spontaneous firing of Purkinje neurons. J Neurosci. 2006 Apr 26;26(17):4602-12.
56. Sacco T, Bruno A, Wanke E, Tempia F. Functional roles of an ERG current isolated in cerebellar Purkinje neurons. J Neurophysiol. 2003 Sep;90(3):1817-28.
57. Paxinos G. The rat nervous system. 3rd ed. Paxinos G, editor. London, UK: Elsevier Academic Press; 2004.

58. Anderson RF. Cerebellar distribution of the dorsal and ventral spinocerebellar tracts in the white rat. J Comp Neurol. 1943;79:415-23.

59. Gerrits NM, Epema AH, van Linge A, Dalm E. The primary vestibulocerebellar projection in the rabbit: absence of primary afferents in the flocculus. Neurosci Lett. 1989 Oct 23;105(1-2):27-33.

60. Arenz A, Bracey EF, Margrie TW. Sensory representations in cerebellar granule cells. Curr Opin Neurobiol. 2009 Aug;19(4):445-51.

61. Bagnall MW, McElvain LE, Faulstich M, du Lac S. Frequency-independent synaptic transmission supports a linear vestibular behavior. Neuron. 2008 Oct 23;60(2):343-52.

62. Barmack NH, Baughman RW, Eckenstein FP. Cholinergic innervation of the cerebellum of rat, rabbit, cat, and monkey as revealed by choline acetyltransferase activity and immunohistochemistry. J Comp Neurol. 1992 Mar 15;317(3):233-49.

63. Kim CH, Oh SH, Lee JH, Chang SO, Kim J, Kim SJ. Lobule-specific membrane excitability of cerebellar Purkinje cells. J Physiol. 2012 Jan 15;590(Pt 2):273-88.

64. Saito Y, Takazawa T, Ozawa S. Relationship between afterhyperpolarization profiles and the regularity of spontaneous firings in rat medial vestibular nucleus neurons. Eur J Neurosci. 2008 Jul;28(2):288-98.

65. Takazawa T, Saito Y, Tsuzuki K, Ozawa S. Membrane and firing properties of glutamatergic and GABAergic neurons in the rat medial vestibular nucleus. J Neurophysiol. 2004 Nov;92(5):3106-20.

66. Sobel EC, Tank DW. In vivo Ca2+ dynamics in a cricket auditory neuron: an example of chemical computation. Science. 1994 Feb 11;263(5148):823-6.

67. Benda J, Longtin A, Maler L. Spike-frequency adaptation separates transient communication signals from background oscillations. J Neurosci. 2005 Mar 2;25(9):2312-21.

68. Wang XJ, Liu Y, Sanchez-Vives MV, McCormick DA. Adaptation and temporal decorrelation by single neurons in the primary visual cortex. J Neurophysiol. 2003 Jun;89(6):3279-93.

69. Rokni D, Tal Z, Byk H, Yarom Y. Regularity, variability and bi-stability in the activity of cerebellar purkinje cells. Front Cell Neurosci. 2009;3:12.

70. Mott DD, Turner DA, Okazaki MM, Lewis DV. Interneurons of the dentate-hilus border of the rat dentate gyrus: morphological and electrophysiological heterogeneity. J Neurosci. 1997 Jun 1;17(11):3990-4005.

71. Goldberg EM, Clark BD, Zagha E, Nahmani M, Erisir A, Rudy B. K+ channels at the axon initial segment dampen near-threshold excitability of neocortical fast-spiking GABAergic interneurons. Neuron. 2008 May 8;58(3):387-400.

72. Gu N, Vervaeke K, Hu H, Storm JF. Kv7/KCNQ/M and HCN/h, but not KCa2/SK channels, contribute to the somatic medium after-hyperpolarization and excitability control in CA1 hippocampal pyramidal cells. J Physiol. 2005 Aug 1;566(Pt 3):689-715.

73. Faber ES, Sah P. Calcium-activated potassium channels: multiple contributions to neuronal function. Neuroscientist. 2003 Jun;9(3):181-94.

74. Scott RH, Sutton KG, Griffin A, Stapleton SR, Currie KP. Aspects of calcium-activated chloride currents: a neuronal perspective. Pharmacol Ther. 1995 Jun;66(3):535-65.

75. Bhattacharjee A, Kaczmarek LK. For K+ channels, Na+ is the new Ca2+. Trends Neurosci. 2005 Aug;28(8):422-8.

76. Benda J, Herz AV. A universal model for spike-frequency adaptation. Neural Comput. 2003 Nov;15(11):2523-64.

77. Peron SP, Gabbiani F. Role of spike-frequency adaptation in shaping neuronal response to dynamic stimuli. Biol Cybern. 2009 Jun;100(6):505-20.

78. Goldberg JM. Afferent diversity and the organization of central vestibular pathways. Exp Brain Res. 2000 Feb;130(3):277-97.

79. Lisberger SG, Miles FA, Optican LM. Frequency-selective adaptation: evidence for channels in the vestibulo-ocular reflex? J Neurosci. 1983 Jun;3(6):1234-44.

80. Kaffashian M, Shabani M, Goudarzi I, Behzadi G, Zali A, Janahmadi M. Profound alterations in the intrinsic excitability of cerebellar Purkinje neurons following neurotoxin 3-acetylpyridine (3-AP)-induced ataxia in rat: new insights into the role of small conductance K(+) channels. Physiol Res. 2010 Nov 29.

국문 초록

서론: 소뇌 퍼킨지 세포는 소뇌피질에서 외부로 정보를 보내는 유일한 세포로서 운동학습에 있어서 매우 중요한 역할을 하는 세포로 알려져 있다. 신경세포는 시냅스 자극이 없는 상태에서도 고유한 흥분성을 가지고 있는 것으로 알려져 있는데, 유입되는 다양한 정보를 처리하여 신경회로망에서 신경세포 고유의 기능을 할 수 있도록 하는 매우 기본적이고 중요한 요소이다. 소뇌 충부는 그 해부학적 위치에 따라 10 개의 소엽으로 나뉘어져 있는데, 각각의 소엽은 그 부위에 따라 소엽-특이적인 감각 정보를 받아들이는 것으로 알려져 있다. 따라서 각각의 소엽을 구성하는 퍼킨지 세포의 내제적 흥분성은 서로 다른 양상을 띨 가능성이 높은데, 아직 이에 대한 연구는 시행된 적이 없다.

방법: 본 연구에서는 패치클램프 방법을 이용하여 척추소뇌 (소엽 III~V)와 전정소뇌 (소엽 X)를 구성하는 퍼킨지 세포의 내재적 흥분성의 차이를 확인하는 것이 그 목표이다.

결과: Whole-cell recording 상황에서 저분극성 전류를 주입하여 주었을 때 나타나는 활동전압 발사 패턴을 보았을 때, 척추소뇌에서는 두가지 종류의 패턴이 관찰되는 반면, 전정소뇌에서는 더 다양하게

네가지 패턴이 관찰되었다. 이 중 gap firing 패턴은 전정소뇌에만 풍부하게 분포하는 A-type K^+ 전류에 의해 발생하는 것으로 확인되었다. 또한 전정소뇌의 퍼킨지 세포는 전류 주입에 따른 반응이 척추소뇌보다 더 넓은 dynamic range 를 나타내었다.

결론: 이처럼 척추소뇌와 전정소뇌를 구성하는 퍼킨지 세포에서 확인되는 내재적 흥분성의 차이는 각기 다른 종류의 감각정보를 처리하는데 특화되어 있기 때문으로 사료된다. 특히 전정소뇌에서 보이는 넓은 dynamic range 는 넓은 범위의 전정자극에도 일정한 효율로 반응할 수 있는 전정계 특유의 성질을 잘 반영한다고 할 수 있겠다.

주요어 : 퍼킨지 세포, 내재적 흥분성, 전정소뇌

학 번 : 2008-31024